

Design, synthesis, and molecular modeling of new 3(2*H*)-pyridazinone derivatives as acetylcholinesterase/butyrylcholinesterase inhibitors

Zeynep Özdemir¹ · Hayriye Yılmaz² · Suat Sarı³ · Arzu Karakurt¹ · Fatma Sezer Şenol⁴ · Mehtap Uysal⁵

Received: 28 December 2016 / Accepted: 22 May 2017 / Published online: 2 June 2017
© Springer Science+Business Media New York 2017

Abstract Inhibition of cholinesterases is an effective method to curb Alzheimer's disease, a progressive and fatal neurological disorder. A series of 6-substituted-3(2*H*)-pyridazinone-2-acetyl-2-(*p*-substituted benzalhidrazone) derivatives were designed, synthesized, and their inhibitory effects on acetylcholinesterase and butyrylcholinesterase were evaluated in pursuit of potent dual inhibitors. We obtained our compounds by the reaction of various substituted/nonsubstituted benzaldehydes with 6-[4-(3,4-dichlorophenyl)piperazine-1-yl]-3(2*H*)-pyridazinone-2-yl acetohydrazide and determined their anticholinesterase activities according to the Ellman's method. **5f** and **5i** showed 75.52 and 71.72% acetylcholinesterase inhibition at 100 µg/ml, respectively. **5h** and **5f**, on the other hand, were the best butyrylcholinesterase inhibitors with 67.16 and 62.03% inhibition at the same concentration, respectively.

5f emerged as a potent dual cholinesterase inhibitor. Through molecular docking studies we predicted the inhibition mechanism of **5f** for both enzymes in comparison with our previous derivatives, which differ in inhibition potency, and tried to get insights into the factors that affect receptor affinity in molecular level.

Keywords AChE inhibitory · BChE inhibitory · 3(2*H*)-Pyridazinone · Benzalhidrazone · Molecular docking

Introduction

Acetylcholinesterase (AChE) and butyrylcholinesterase (BChE) are known serine hydrolase enzymes responsible for the hydrolysis of acetylcholine (ACh), which is a significant neurotransmitter for regulation of cognition in animals (Saeed et al. 2014; Shah et al. 2016; Chiou et al. 2009; Tampi et al. 2016; Bentley et al. 2011). BChE can also hydrolyse some esters different from ACh, but the role of this enzyme is less known (Groner et al. 2007; Chiou et al. 2009). Inhibition of these enzymes leads to the rise of ACh levels in cholinergic synapses (Groner et al. 2007). Thus, cholinesterase inhibitors are used in the treatment of various neuromuscular disorders which occur as a result of reduced cortical and hippocampal levels of ACh such as Alzheimer's disease (AD). AD is a complex neurodegenerative disorder characterized by synapse dysfunction, neuronal death, and loss of memory and learning ability (Candeias et al. 2012; Cacabelos 2008; Strelnik et al. 2016; Gilhus et al. 2016). Current treatment approaches for AD continue to be principally symptomatic, with the major therapeutic strategy based on the relationship between the observed cholinergic

Electronic supplementary material The online version of this article (doi:10.1007/s00044-017-1930-x) contains supplementary material, which is available to authorized users.

✉ Zeynep Özdemir
zeynep.bulut@inonu.edu.tr
zpozdmr@gmail.com

¹ Faculty of Pharmacy, Department of Pharmaceutical Chemistry, Inonu University, Malatya 44280, Turkey

² Kayseri Vocational School, Department of Biomedical Devices and Technologies, Erciyes University, Kayseri 38039, Turkey

³ Faculty of Pharmacy, Department of Pharmaceutical Chemistry, Hacettepe University, Ankara 06100, Turkey

⁴ Faculty of Pharmacy, Department of Pharmacognosy, Gazi University, Ankara 06100, Turkey

⁵ Faculty of Pharmacy, Department of Pharmaceutical Chemistry, Gazi University, Ankara 06100, Turkey

dysfunction and AD, known as the cholinergic hypothesis, and specifically on cholinesterase inhibition (Anand and Singh 2013; Ballard et al. 2011).

Various AChE inhibitors such as tacrine, donepezil, rivastigmine, and galantamine (Fig. 1) have been used contemporarily for the symptomatic treatment of AD (Mehta et al. 2012; Zha et al. 2016; Williams et al. 2011; Cummings et al. 2007; Costanzo et al. 2016; Romero et al. 2013; Camps et al. 2008). In recent years, novel cholinesterase inhibitors from natural resources or synthetic ways, which have coumarin, benzofuran, berberine, β -carboline, benzophenone, ferulic acid, naphthyridine, triazine, and quinolone scaffolds as the main pharmacophoric groups, have been reported (Saeed et al. 2015; Delogu et al. 2016; Jiang et al. 2011; Otto et al. 2014; Huang et al. 2012; Belluti et al. 2011; Catto et al. 2012; Chen et al. 2012; Samadi et al. 2012).

Although BChE is sparsely expressed, recent studies proved that AChE inhibition alone may not be sufficient to impair cholinesterase activity and elevate choline levels since BChE makes up for the lost AChE activity. Furthermore, it is known that BChE expression is increased during AD (Mesulam et al. 2002; Li et al. 2008).

With the recent crystallographic studies structural features of AChE and BChE active sites have been clearer and the binding interactions of known inhibitors like tacrine, donepezil, and galantamine with the key binding site residues are well studied (Dvir et al. 2010; Nicolet et al. 2003; Nachon et al. 2013; Leon and Marco-Contelles 2011; Simoni et al. 2012; Nepovimova et al. 2014; Cheung et al. 2012). Donepezil, unlike galantamine and tacrine, interacts with the so-called peripheral anionic site (PAS) residues which line the rim at the entrance of the active gorge as well

as the cationic active site (CAS) and acyl-binding pocket (Costanzo et al. 2016; Cheung et al. 2012; Camps et al. 2009; Bourne et al. 2003; Tougu 2001). At the bottom of this gorge are three amino acids, which catalyse the cleavage of acetyl-choline bond, namely S203, E334, and H447, also known as the catalytic triad (Zhou et al. 2010). Ideally, a cholinesterase inhibitor is expected to effectively interact with these sites (Fig. 2). Although the active site gorge residues of BChE and AChE share 65% sequence identity some differences are critical to enzyme specificity such as the volume of the acyl-binding pocket, which is larger in BChE (Brus et al. 2014).

3(2*H*)-pyridazinone derivatives were claimed to possess diverse bioactivities such as antibacterial, antifungal, anti-tuberculosis, analgesic, anti-inflammatory, antihypertensive, anticancer, anticholinesterase, and antioxidant activities (Nagle et al. 2014; Utku et al. 2011a, 2011b; Şahin et al. 2004; Siddiqui et al. 2010, 2011; Yamali et al. 2015; Rathish et al. 2012; Abd El-Ghaffar et al. 2011). The contribution to the activity of aryl substituents at the sixth

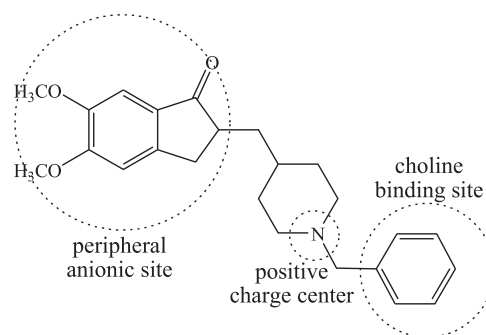
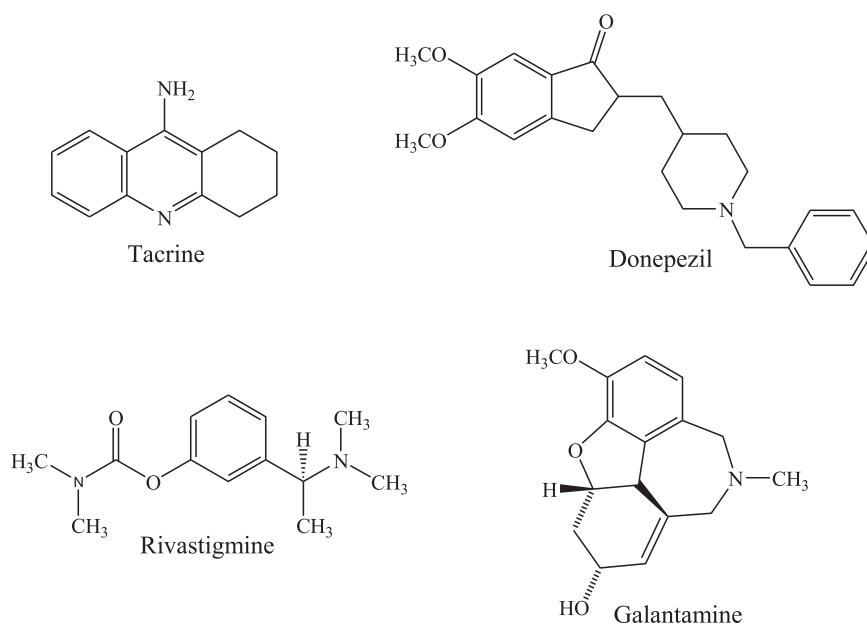


Fig. 2 Structural hypothesis for AChE inhibitors

Fig. 1 Molecular structure of tacrine, donepezil, rivastigmine, and galantamine



position of 3(2*H*)-pyridazinone was investigated in many studies (Utku et al. 2011a, 2011b; Şahin et al. 2004; Yamali et al. 2015; Rathish et al. 2012; Abd El-Ghaffar et al. 2011; Xing et al. 2013). In a late study, Xing et al. (2013) identified high affinity AChE inhibitors in 2,6-disubstituted pyridazinone structure. In a previous study, we reported a series of 3(2*H*)-pyridazinone derivatives bearing ethyl propionate and propylhydrazone at the second position of pyridazinone with AChE/BChE inhibitory activities (Özçelik et al. 2010). Later we reported a series of 6-substituted-3(2*H*)-pyridazinone derivatives among which **5u** and **5v** were found to have potent AChE inhibitory activity (Önkol et al. 2013; Utku et al. 2011a, 2011b) (Fig. 3).

In view of the above mentioned findings we designed and synthesized 18 new 6-(4-(3,4-dichlorophenyl)piperazine-1-yl)-3(2*H*)-pyridazinone-2-acetyl-2-(substitutedbenzal) hydrazone derivatives (**5a–t**) and in vitro evaluated their AChE and BChE inhibitory effects by using Ellman's method, which is the most commonly used method to measure cholinesterase activity. It is especially useful in monitoring disulphide bond formation in solution phase reactions. The Ellman method is also useful in testing the quality of peptides containing free sulfhydryl groups (Ellman et al. 1961).

The choline-binding site moiety was designed as a 3,4-dichlorophenyl ring and the structural modifications were focused on substitutions on the phenyl ring of acetobenzalhydrazone moiety. Methyl, methoxy, chloro, bromo, fluoro, nitro, amino, and cyano groups were included as substitutions on this ring at varying positions and combinations. Using molecular docking approach we tried to get insights into binding interactions of our derivatives in comparison with **5u** and **5v** in the active site of both enzymes and understand the facts that underlie the relationships between structural modifications on these ligands and their efficacy.

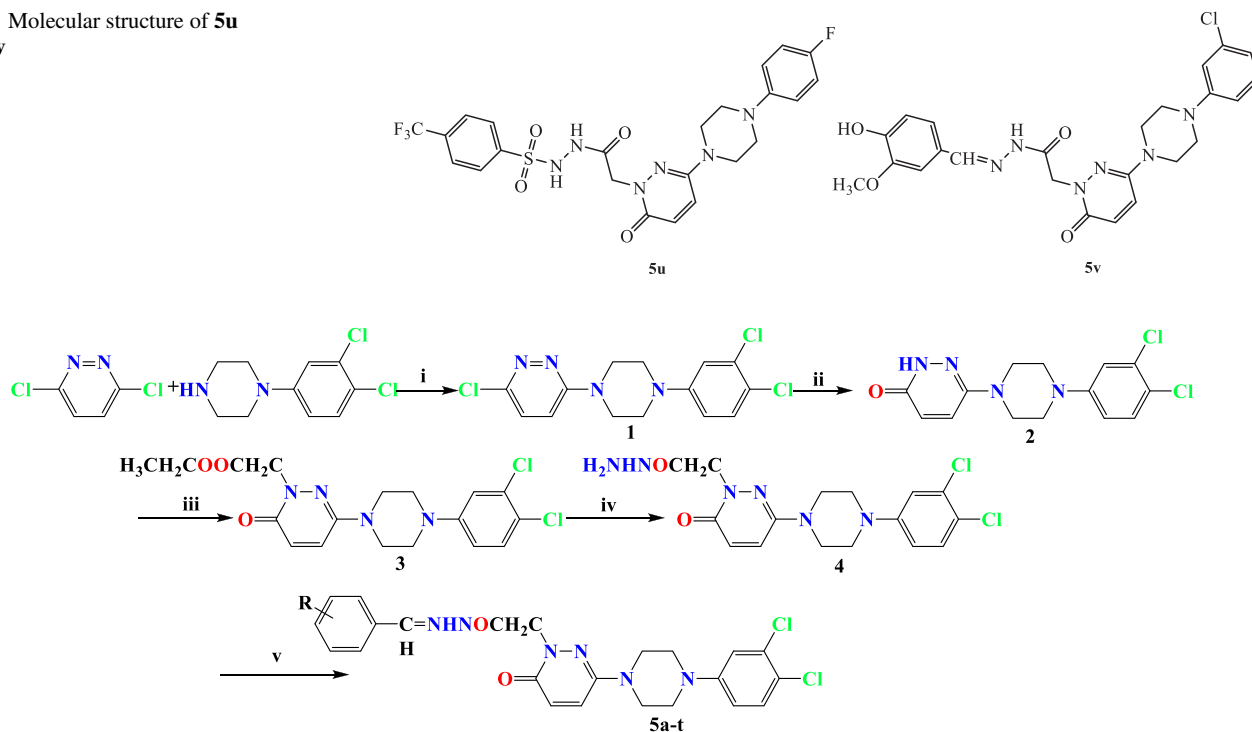
Results and discussion

Chemistry

5a–t were synthesized according to the literature methods as outlined in Scheme 1.

Nucleophilic displacement reaction of commercial 3,6-dichloropyridazine with 3,4-dichlorophenylpiperazine in ethanol afforded 3-chloro-6-substitutedpyridazine (**1**). 6-(4-(3,4-dichlorophenyl)piperazine-1-yl)-3(2*H*)-pyridazinone

Fig. 3 Molecular structure of **5u** and **5v**



(i) EtOH, reflux (6h); (ii) AcOH, reflux (6h); (iii) BrCH₂COOCH₂CH₃, K₂CO₃, acetone, reflux (24h), (iv) H₂NNH₂·H₂O, MeOH, stirred in rt (3h); (v) ArCHO, EtOH, reflux (6h)

R: -H, 4-Br, 2-Cl, 4-Cl, 4-F, 3-CH₃, 4-CH₃, 2-OCH₃, 3-OCH₃, 4-OCH₃, 2,3-diOCH₃, 3,5-diOCH₃, 2,4,6-triOCH₃, 3,4,5-triOCH₃, 4-N(CH₃)₂, 4-NO₂, 2-CN, 3-CN

Scheme 1 Synthesis of the compounds

(2) was obtained as a result of hydrolysis of 3-chloro-6-[4-(3,4-dichlorophenyl)piperazine-1-yl]pyridazine by heating in glacial acetic acid (Şahin et al. 2004). Ethyl 6-(3,4-dichlorophenyl)piperazine-1-yl-3(2*H*)-pyridazinone-2-ylacetate (3) was obtained by the reaction of 2 with ethyl bromoacetate in the presence of K_2CO_3 in acetone (Şahin et al. 2004). Then, 6-(3,4-dichlorophenyl)piperazine-1-yl-3(2*H*)-pyridazinone-2-ylacetohydrazide (4) was synthesized by the condensation reaction of 3 with hydrazine hydrate (99%) (Şahin et al. 2004). Ultimately, the title compounds bearing benzalhydrazone structure were obtained by the reaction of 4 with substituted/non-substituted benzaldehydes. 2–4 and 5a–t were reported for the first time in this study. The reaction yields of the compounds range approximately from 50 to 90%. Compound 5k was synthesized with the highest yield (93%) while compound 5d was the compound synthesized with the lowest yield (56%). Molecular structures of 2–4 were confirmed by infrared (IR) and 1H -NMR and 5a–t by IR, 1H -NMR, ^{13}C -NMR, and mass spectral data. Molecular structures, yields, melting points, molecular weights, and molecular formula of 5a–t are given in Table 1.

Anticholinesterase activity

In vitro AChE and BChE inhibition of 5a–t was determined by the method of Ellman et al. (1961) using galantamine as reference and the activity data of the compounds were summarized as percentage inhibition \pm standard deviation (SD) values at 100 μ g/ml concentration in Table 2. All compounds showed significant inhibitory activity against AChE and BChE with higher inhibition trend against the former except 5h. The inhibition % of 5g and 5r could not be measured because of collapse. 5f and 5i, 3-methyl benzalhydrazone and 3-methoxybenzalhydrazone derivatives, showed the best AChE inhibition with 75.52 and 71.72%. On the other hand 5h, 2-metoxibenzalhydrazone derivative, and 5f exhibited the highest inhibitory effect against BChE with 67.16 and 62.03% inhibition, respectively. Thus, 5f emerged as a promising dual cholinesterase inhibitor lead molecule. In general, substitution on benzalhydrazone phenyl ring lead to an increase in AChE and BChE inhibition. Substitutions on the *meta* position of the benzalhydrazone phenyl ring with $-OCH_3$ and $-CH_3$ also improved the anti-AChE activity. Adversely, *p*-substitution on the benzalhydrazone phenyl ring with strong electron-donating groups such as $-OCH_3$ was observed to reduce the AChE inhibition.

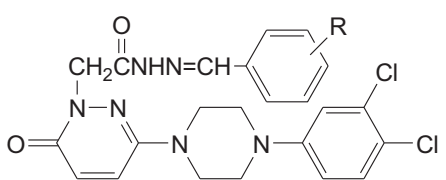
Molecular docking studies

Glide predicted good fit for 5f in the active site of human AChE (PDB code 4EY7) along the gorge with some

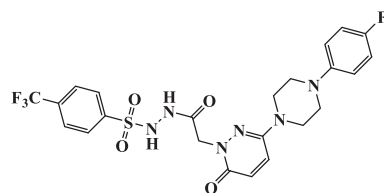
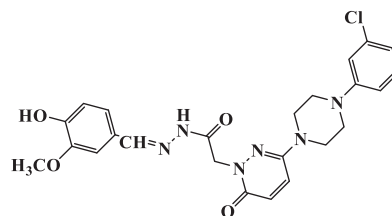
characteristic interactions previously defined for some known inhibitors (Fig. 4a). The 3,4-dichlorophenyl moiety of 5f occupied the choline-binding pocket and engaged in strong π - π stacking against W86 aromatic side chain and weak interactions with E202 and the catalytic residue H447. These residues are reportedly involved in ligand–receptor complexes of tacrine, galantamine, huperzine A, and donepezil (Nachon et al. 2013; Cheung et al. 2012). The piperazine ring occupied the acyl-binding pocket entrance and the constriction site beneath PAS contacting Y124, Y337, and F338 aromatic side chains. Donepezil was reported to form water-mediated H-bonds with Y337 and Y341 via its quaternary *N* of the piperidine ring (Fig. 4d). Probably the key difference between our derivatives and donepezil is that our derivatives are non-ionized at physiological pH hence the absence of such interaction. Instead, via its carbonyl oxygen of the pyridazinone ring, 5f formed a water-mediated H-bond to R296 backbone NH and a direct H-bond to F295 backbone NH. The latter interaction was reportedly observed with the carbonyl oxygen of the indanone moiety of donepezil (Cheung et al. 2012). The pyridazinone ring of 5f occupied the lower PAS and π - π stacked with Y341 aromatic side chain. In the upper PAS, the 3-methylbenzene ring positioned in the space between W286 and Y72 making hydrophobic contacts.

5u and 5v, two structural analogues of 5f, were previously synthesised and their AChE inhibitory activities were screened. 5u was reported to show $74.27 \pm 0.78\%$ AChE inhibition at 0.25 mM, which is very close to 5f's molar inhibition (75.52% at 0.199 mM). On the other hand 5v was reported to show greater inhibition for the same enzyme with $99.76 \pm 1.54\%$ at 0.2 mM. Glide predicted 5u's binding mode and interactions in human AChE active site very similar to 5f (Fig. 4b) whereas 5v's docking solution differed from those of 5u and 5f to some extent (Fig. 4c). Upon close inspection of these receptor–ligand complexes one can see that the 4-fluorobenzene ring of 5v is slightly flipped and stacked with W337 aromatic side chain and it does not reach as deep to the bottom of the gorge as the 3,4-dichlorobenzene and 4-chlorobenzene of 5f and 5u, respectively. This way the 4-trifluorobenzene ring of 5v lays over the rim of the active site gorge entrance lined by Y72 and T75. The chlorine atoms of 5f and 5u occupying the choline binding pocket, as they are bulkier than the fluorine on 4-fluorobenzene of 5v, make unfavourable VdW interactions, i.e., bad contacts, with some of the residues lining the bottom of the active site gorge (Fig. 5). Thus, 4-*F* appears a good substitution on this benzene ring with its relatively small volume and high electron affinity. Additionally, Glide scores of these derivatives were in line with their in vitro inhibition percentages (Table 3).

We docked these compounds in human BChE active site gorge as well (PDB code 4BDS) and observed similarities

Table 1 Molecular structures, yields, melting points, molecular weights, and molecular formula of **5a–t**


Compound	R	Yield (%)	MP (°C)	MW (g/mol)	Molecular formula
5a	–H	70	278–80	485.37	C ₂₃ H ₂₂ Cl ₂ N ₆ O ₂
5b	4-Br	87	271–3	564.26	C ₂₃ H ₂₁ BrCl ₂ N ₆ O ₂
5c	2-Cl	81	267–9	519.81	C ₂₃ H ₂₁ Cl ₃ N ₆ O ₂
5d	4-Cl	56	275–7	519.81	C ₂₃ H ₂₁ Cl ₃ N ₆ O ₂
5e	4-F	84	228–30	503.36	C ₂₃ H ₂₁ Cl ₂ FN ₆ O ₂
5f	3-CH ₃	79	297–9	499.39	C ₂₄ H ₂₄ Cl ₂ N ₆ O ₂
5g	4-CH ₃	81	255–7	499.39	C ₂₄ H ₂₄ Cl ₂ N ₆ O ₂
5h	2-OCH ₃	86	263–5	515.39	C ₂₄ H ₂₄ Cl ₂ N ₆ O ₃
5i	3-OCH ₃	80	258–60	515.39	C ₂₄ H ₂₄ Cl ₂ N ₆ O ₃
5k	4-OCH ₃	93	228–30	515.39	C ₂₄ H ₂₄ Cl ₂ N ₆ O ₃
5l	2,3-diOCH ₃	75	265–7	545.42	C ₂₅ H ₂₆ Cl ₂ N ₆ O ₄
5m	3,5-diOCH ₃	65	271–3	545.42	C ₂₅ H ₂₆ Cl ₂ N ₆ O ₄
5n	2,4,6-triOCH ₃	61	273–5	575.44	C ₂₆ H ₂₈ Cl ₂ N ₆ O ₅
5o	3,4,5-triOCH ₃	67	286–8	575.44	C ₂₆ H ₂₈ Cl ₂ N ₆ O ₅
5p	4-N(CH ₃) ₂	78	284–6	528.43	C ₂₅ H ₂₇ Cl ₂ N ₇ O ₂
5r	4-NO ₂	85	207–9	530.36	C ₂₃ H ₂₁ Cl ₂ N ₇ O ₄
5s	2-CN	88	236–8	510.38	C ₂₄ H ₂₁ Cl ₂ N ₇ O ₂
5t	3-CN	65	273–5	510.38	C ₂₄ H ₂₁ Cl ₂ N ₇ O ₂
5u*					

**5v****

* (Utku et al. 2011a, 2011b)

** (Önkol et al. 2013)

with their binding modes in AChE active site (Fig. 6a). Our derivatives lack substitutions to fill the relatively larger acyl-binding pocket and interact with W231, L286, and V288 (Fig. 6b), which might account for their relatively

lower BChE inhibition percentages. Indeed, some selective BChE inhibitors with nanomolar IC₅₀ values were reported to effectively occupy this midgorge (Kneza et al. 2015). The 2,4-dichlorobenzene moiety of **5f** again occupied the

Table 2 AChE and BChE inhibition values (%) of the title compounds at 100 µg/ml

Compound	AChE inhibition (Inhibition ± SD*)	BChE inhibition (Inhibition ± SD)
5a	43.82 ± 2.36	19.27 ± 1.56
5b	58.17 ± 0.74	42.44 ± 3.33
5c	53.13 ± 2.30	31.03 ± 1.05
5d	65.55 ± 3.26	47.58 ± 3.09
5e	64.95 ± 4.36	46.71 ± 1.61
5f	75.52 ± 1.76	62.03 ± 1.82
5g	**	**
5h	61.70 ± 1.66	67.16 ± 1.29
5i	71.72 ± 0.01	54.98 ± 1.69
5k	41.69 ± 1.38	21.91 ± 3.62
5l	64.19 ± 2.72	52.60 ± 2.76
5m	60.18 ± 3.94	43.81 ± 0.90
5n	68.01 ± 2.84	44.05 ± 5.70
5o	65.85 ± 1.32	55.14 ± 1.28
5p	66.77 ± 1.54	58.20 ± 2.45
5r	**	**
5s	63.72 ± 5.70	8.87 ± 3.01
5t	49.19 ± 1.07	28.54 ± 3.57
Galantamine	95.68 ± 1.30	83.89 ± 1.06

* Standard deviation

** percent inhibition for **5g** and **5r** could not be determined due to precipitation during the assay

choline-binding subdomain, π - π stacked with W82 aromatic side chain, made π -cation interaction with the imidazolium of H438 (counterpart of H447 in AChE catalytic triad), and formed halogen bond with Y128 side chain via 4-Cl. The carbonyl oxygen of the acetylhydrazone function made a water-mediated H-bond with N70 in PAS.

Conclusion

As a continuation of our research interest in developing novel 3(2*H*)-pyridazinone derivative anticholinesterase compounds and establishing new relationships between their structure and activity, we designed and synthesized a series of 6-(4-(3,4-dichlorophenyl)piperazine-1-yl)pyridazin-3(2*H*)-pyridazinone-2-acetyl-3-(*p*-substituted/ non-substituted benzal)hydrazone derivatives and evaluated their AChE and BChE inhibitory activities according to the Ellman's method. Compounds with significant inhibition at 100 µg/ml were obtained. Compound **5f** emerged as a potent dual inhibitor with 75.52 ± 1.76 and 62.03 ± 1.82% inhibition against AChE and BChE, respectively. It was less potent than the reference drug galantamine, yet promising for further modifications as a lead. The molecular docking

studies showed similarities in binding interactions in active site gorges of the enzymes with known inhibitors, such as donepezil. However 3,4-dichloro substitution on the phenyl of the 4-phenylpiperazine moiety was sterically less favourable in comparison with 4-fluoro substitution, which is thought to be the reason for **5v**'s higher efficacy. Lower inhibition rates against BChE was probably due to the failure in effectively filling the larger acyl-binding pocket of this enzyme's active site gorge.

Experimental

Chemistry

All chemicals were purchased from Aldrich, Fluka AG, and E. Merck. The purity of all compounds was checked by thin layer chromatography with Merck Kieselgel F₂₅₄ plates. Melting points were determined on Electrothermal 9200 melting points apparatus and the values were uncorrected. IR spectra were recorded on a Perkin Elmer Spectrometer by attenuated total reflection (ATR) technique. ¹H-NMR and ¹³C-NMR spectra were recorded on a Bruker Avance Ultrashield FT-NMR spectrometer in DMSO and CDCl₃ at 300 MHz in Inonu University, Malatya. The mass spectra (HRMS) of the compounds were recorded on Waters Acquity Ultra Performance Liquid Chromatography Micromass and combined with LCT Premier™ XE UPLC/MS TOFF spectrophotometer (Waters Corp, Milford, USA) by ESI+ and ESI- techniques.

Synthesis of 6-(4-(3,4-dichlorophenyl)piperazine-1-yl)-3(2*H*)-pyridazinone (2)

A solution of 0.05 mol of a 6-substituted-3-chloropyridazinone derivative (**1**) in 30 ml glacial acetic acid was refluxed for 6 h. Acetic acid was removed under reduced pressure, the residue was dissolved in water and extracted with chloroform. The organic phase was dried over sodium sulphate and evaporated under reduced pressure. The residue was purified by recrystallization from ethanol (Utku et al. 2011a, 2011b).

Synthesis of ethyl 6-(4-(3,4-dichlorophenyl)piperazine-1-yl)-3(2*H*)-pyridazinone-2-ylacetate (3)

A mixture of 0.01 mol 6-(4-(3,4-dichlorophenyl)piperazine-1-yl)-3(2*H*)-pyridazinone (**2**), 0.02 mol ethyl bromoacetate, and 0.02 mol potassium carbonate in acetone (40 ml) was refluxed overnight. After the mixture was cooled, the organic salts were filtered off, the solvent was evaporated, and the residue was purified by recrystallization with methanol to give the esters (Utku et al. 2011a, 2011b).

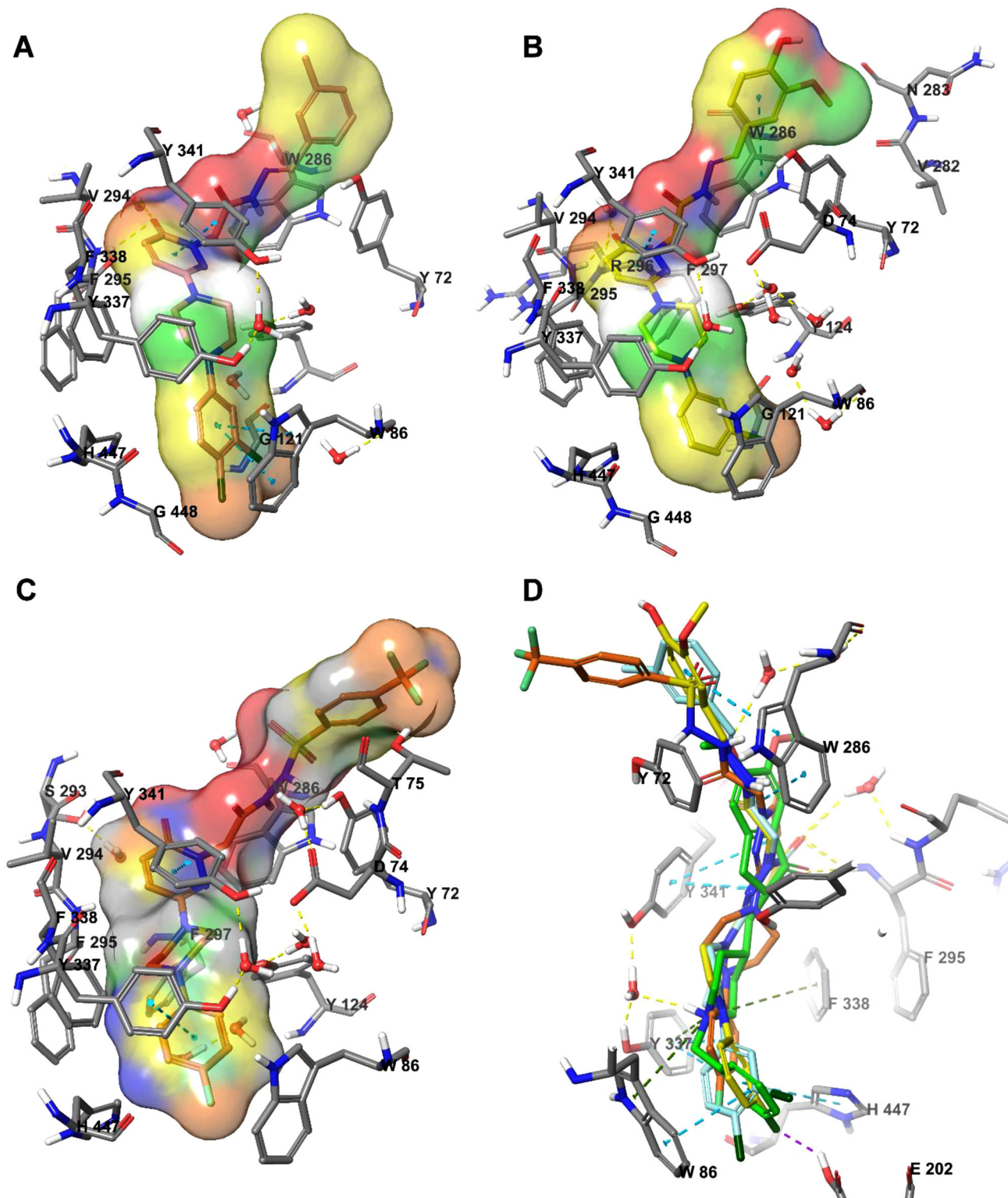


Fig. 4 Binding modes of **5f** (a), **5u** (b), **5v** (c), and donepezil superimposed with the rest in AChE active site gorge. Side views of the active site show ligands and binding-site residues as grey and colour

sticks, water molecules as stick and balls; ligand molecular surfaces as solid, partial-charge coloured; H-bonds (yellow) and π - π stacks (turquoise) as dashed lines (color figure online)

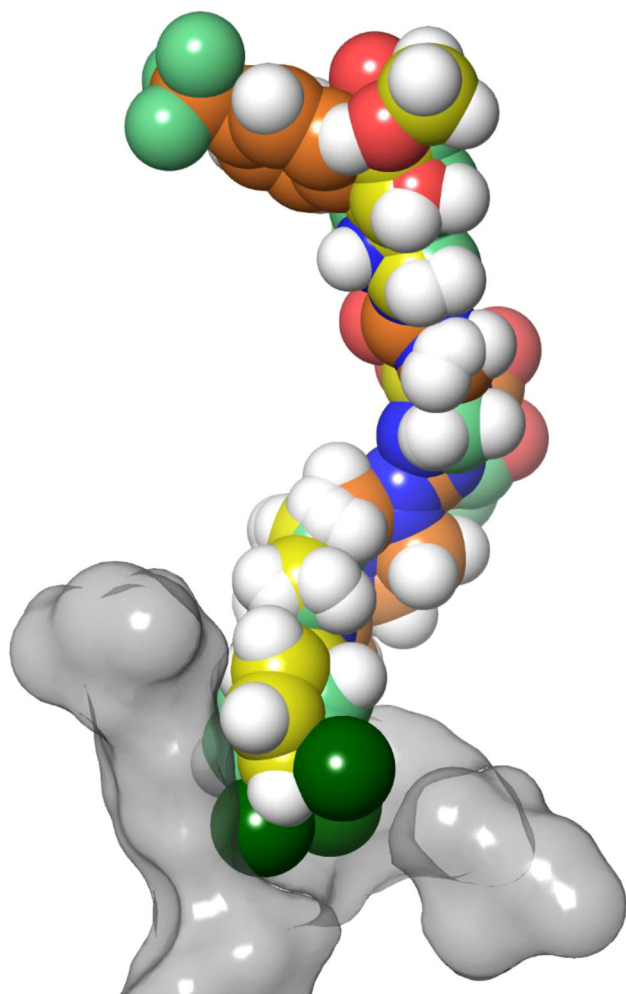


Fig. 5 Binding modes of **5f** (aquamarine), **5u** (yellow), and **5v** (orange) in AChE active site gorge. Side view of the gorge showing ligands as colour CPK and the molecular surface of the lower gorge residues as opaque grey (color figure online)

Table 3 Glide scores (kcal/mol) of **5f**, **5u**, **5v** in AChE and BChE active sites

Compound	AChE	BChE
5f	−7.50	−7.28
5u	−7.23	−6.54
5v	−8.11	−9.02

Synthesis of ethyl 6-(4-(3,4-dichlorophenyl)piperazine-1-yl)-3(2H)-pyridazinone-2-ylacetohydrazide (**4**)

Hydrazine hydrate (99%, 3 ml) was added to the solution of 0.01 mol ethyl 6-(4-(3,4-dichlorophenyl)piperazine-1-yl)-3(2H)-pyridazinone-2-ylacetate (**3**) in 25 ml methanol and

stirred for 3 h at room temperature. The precipitate obtained was filtered off, washed with water, dried, and recrystallized from ethanol (Şahin et al. 2004).

General procedure for the preparation of 6-(4-(3,4-dichlorophenyl)piperazine-1-yl)-3(2H)-pyridazinone-2-acetyl-2-(substitutedbenzal)hydrazones (**5a–t**)

0.01 mol 6-(4-(3,4-dichlorophenyl)piperazine-1-yl)-3(2H)-pyridazinone-2-yl acetohydrazide (**4**) and 0.01 mol substituted/nonsubstituted benzaldehyde were stirred in ethanol (15 ml) and refluxed for 6 h. At the end of the reaction, the mixture was poured into ice water. The precipitate was filtered, dried, and crystallized from methanol/water (Şahin et al. 2004).

6-(4-(3,4-dichlorophenyl)piperazine-1-yl)-3(2H)-pyridazinone (**2**)

White crystals; yield: 91.67%; mp: 253–255 °C; IR (ν cm^{-1} , ATR): 3444 (N–H), 3020 (C–H aromatic), 2923 (C–H aliphatic), 1679 (C=O), 1586 (C=N), 1238 (C–N), 1006 (C–O) and 831 (C–Cl); $^1\text{H-NMR}$ (CDCl_3 -*d*, 300 MHz): δ (ppm) 3.34 (4H; t; CH_2 -N; piperazine b + b'), 3.45 (4H; t; CH_2 -N; piperazine a + a'), 6.84 (1H; d; pyridazinone H⁵), 6.87 (1H; d; pyridazinone H⁴), 7.10–7.32 (3H; m; phenyl protons) and 10.42 (1H; s; –NH). $^{13}\text{C-NMR}$ ($\text{DMSO-}d_6$, 400 MHz), δ 45.99 (2C; CH_2 -N), 47.13 (2C; CH_2 -N), 115.56 (1C; pyridazinone C⁵), 116.54 (1C; pyridazinone C⁴), 119.91 (1C; 3,4-dichlorophenyl C⁶), 127.11 (1C; 3,4-dichlorophenyl C²) 130.46 (1C; 3,4-dichlorophenyl C⁵), 131.03 (1C; 3,4-dichlorophenyl C¹), 131.50 (1C; pyridazinone C⁶), 149.05 (1C; 3,4-dichlorophenyl C⁴), 150.56 (1C; 3,4-dichlorophenyl C³), and 158.88 (1C; pyridazinone C³); $\text{C}_{14}\text{H}_{14}\text{Cl}_2\text{N}_4\text{O}$ MS (ESI+) calculated: 324.05, Found: *m/e* 325.0588 (M^+ ; 100.0%) and 327.0587 (M^{+2} ; 67.9%).

Ethyl 6-(4-(3,4-dichlorophenyl)piperazine-1-yl)-3(2H)-pyridazinone-2-ylacetate (**3**)

White crystals; yield: 57.79%; mp: 212–214 °C; IR (ν cm^{-1} , ATR): 3064 (C–H aromatic), 2981 (C–H aliphatic), 1753 (C=O ester), 1665 (C=O), 1588 (C=N), 1236 (C–N), 1027 (C–O) and 843 (C–Cl); $^1\text{H-NMR}$ (CDCl_3 -*d*, 300 MHz): δ (ppm) 1.31 (3H; t; – CH_3), 3.30 (4H; t; CH_2 -N; b + b'), 3.41 (4H; t; CH_2 -N; a + a'), 4.22 (2H; q; –O– CH_2 –), 4.78 (2H; s; –N– CH_2 –C=O), 6.78 (1H; d; pyridazinone H⁵), 6.80 (1H; d; pyridazinone H⁴) and 6.92–7.34 (3H; m; phenyl protons). $^{13}\text{C-NMR}$ ($\text{DMSO-}d_6$, 400 MHz), δ 14.13 (1C; CH_3), 46.39 (2C; CH_2 -N), 48.63 (2C; CH_2 -N), 52.89 (1C; –N– CH_2 –C=O), 61.54 (1C; – OCH_2 –), 115.98 (1C; pyridazinone C⁵), 117.94 (1C; 3,4-dichlorophenyl C⁶),

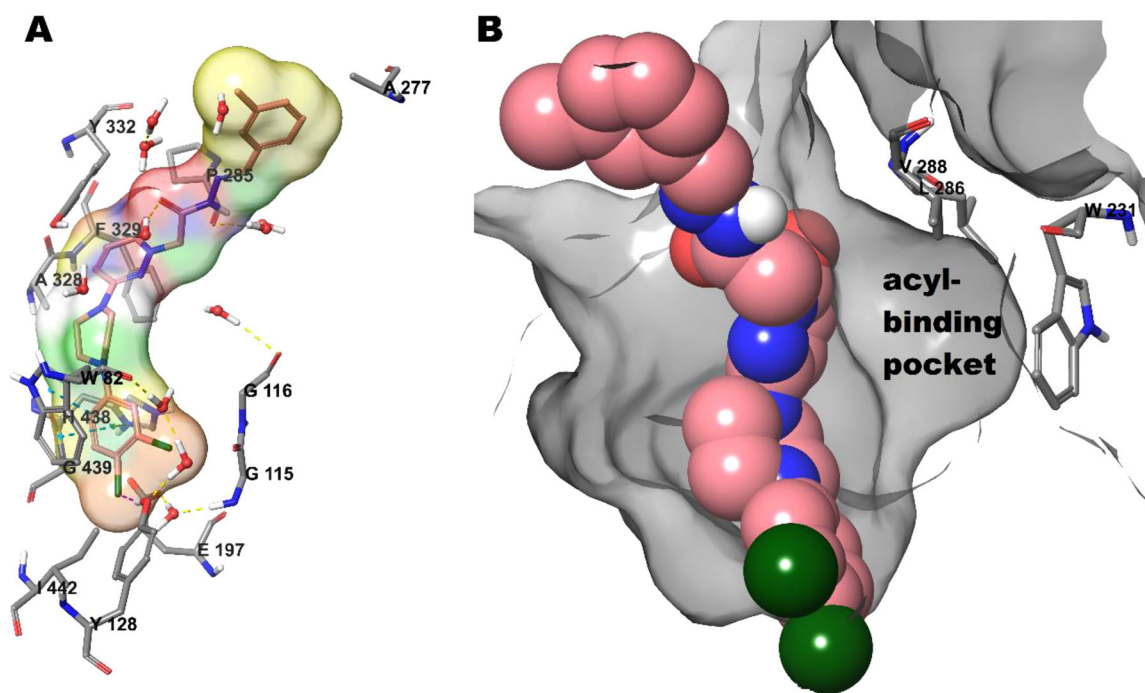


Fig. 6 Binding mode of **5f** in BChE active site gorge. Side views of the active site show **a 5f** and binding-site residues as grey and colour sticks, water molecules as stick and balls; **5f** molecular surface as solid, partial-charge coloured; H-bonds (yellow), π - π stacks

(turquoise), and cation- π interaction (green) as dashed lines; **b 5f** in colour CPK, acyl-binding pocket residues in grey sticks, and receptor surface in transparent solid grey. Chlorine atoms are again protruding through the receptor surface (color figure online)

125.96 (1C; pyridazinone C⁴), 126.84 (1C; 3,4-dichloro-phenyl C²), 130.62 (1C; 3,4-dichlorophenyl C⁵), 131.31 (1C; 3,4-dichlorophenyl C¹), 132.98 (1C; pyridazinone C⁶), 148.66 (1C; 3,4-dichlorophenyl C⁴), 150.01 (1C; 3,4-dichlorophenyl C³), 158.38 (1C; pyridazinone C³) and 167.74 (1C; CH₂-N-C=O); C₁₈H₂₀Cl₂N₄O₃ MS (ESI+) calculated: 410.09, Found: *m/e* 411.0990 (M⁺; 100.0%) and 413.0984 (M⁺²; 67.9%).

6-(4-(3,4-Dichlorophenyl)piperazine-1-yl)-3(2H)-pyridazinone-2-ylacetohydrazide (4)

White crystals; yield: 78.23%; mp: 207–209 °C; IR (ν cm⁻¹, ATR): 3308 (N-H), 3056 (C-H aromatic), 2837 (C-H aliphatic), 1682 (C=O), 1590 (C=N), 1235 (C-N) and 846 (C-Cl); ¹H-NMR (CDCl₃-*d*, 300 MHz): δ (ppm) 3.27 (4H; t; CH₂-N; b + b'), 3.46 (4H; t; CH₂-N; a + a'), 4.74 (2H; s; -N-CH₂-C=O), 5.15 (2H; s; -NH₂), 6.79 (1H; d; pyridazinone H⁵), 6.81 (1H; d; pyridazinone H⁴), 6.94–7.35 (3H; m; phenyl protons) and 7.75 (1H; s; -NH-N). ¹³C-NMR (DMSO-*d*₆, 400 MHz), δ 45.67 (2C; CH₂-N), 47.07 (2C; CH₂-N), 52.16 (1C; -N-CH₂-C=O), 116.56 (1C; pyridazinone C⁵), 119.94 (1C; 3,4-dichlorophenyl C⁶), 126.55 (1C; pyridazinone C⁴), 130.64 (1C; 3,4-dichlorophenyl C²), 131.51 (1C; 3,4-dichlorophenyl C⁵), 148.51 (1C; 3,4-dichlorophenyl C¹), 150.55 (1C; pyridazinone C⁶), 157.66 (1C; 3,4-dichlorophenyl C⁴), 158.90

(1C; 3,4-dichlorophenyl C³), 166.25 (1C; CH₂-N-C=O) and 168.10 (1C; pyridazinone C³); C₁₆H₁₈Cl₂N₆O₂ MS (ESI+) calculated: 396.09, Found: *m/e* 397.0909 (M⁺; 100.0%), 399.0906 (M⁺²; 67.9%) and 402.0923 (M⁺⁴; 10.2%).

6-(4-(3,4-Dichlorophenyl)piperazine-1-yl)-3(2H)-pyridazinone-2-acetyl-2-(benzal)hydrazon (5a)

White crystals; yield: 70.25%; mp: 278–280 °C; IR (ν cm⁻¹, ATR): 3676 (N-H), 3065 (C-H aromatic), 2901 (C-H aliphatic), 1693 (C=O), 1569 (C=N), 1237 (C-N) and 844 (C-Cl); ¹H-NMR (DMSO-*d*₆, 300 MHz): δ (ppm) 2.51 (4H; t; CH₂-N; b + b'), 3.30 (4H; t; CH₂-N; a + a'), 5.06 (2H; s; -N-CH₂-C=O), 6.93 (1H; d; pyridazinone H⁵), 6.97 (1H; d; pyridazinone H⁴), 7.00–7.71 (8H; m; phenyl protons), 8.02 (1H; s; -N=CH-) and 11.66 (1H; s; -NH-N); ¹³C-NMR (DMSO-*d*₆, 300 MHz), δ 46.20 (2C; CH₂-N), 47.63 (2C; CH₂-N), 78.91 (1C; -N-CH₂-C=O), 116.08 (1C;=CH), 117.05 (1C; pyridazinone C⁵), 120.57 (1C; 3,4-dichlorophenyl C⁶), 127.05 (1C; 3,4-dichlorophenyl C⁵), 127.31 (1C; pyridazinone C⁴), 129.22–130.90 (5C; phenyl C²⁻⁶), 132.02 (1C; 3,4-dichlorophenyl C²) 134.41 (1C; phenyl C¹), 144.36 (1C; 3,4-dichlorophenyl C¹), 148.96 (1C; pyridazinone C⁶), 150.98 (2C; 3,4-dichlorophenyl C^{3,4}), 158.31 (1C; CH₂-N-C=O) and 168.40 (1C; pyridazinone C³); C₂₃H₂₂Cl₂N₆O₂ MS (ESI+)

calculated: 484.12, Found: *m/e* 485.1262 (M^+ ; 100.0%), 487.1226 (M^{+2} ; 67.9%) and 488.1237 (M^{+4} ; 10.2%).

6-(4-(3,4-Dichlorophenyl)piperazine-1-yl)-3(2H)-pyridazinone-2-acetyl-2-(4-bromobenzal)hydrazon (**5b**)

White crystals; yield: 87.56%; mp: 271–273 °C; IR (ν cm^{-1} , ATR): 3091 (C–H aromatic), 2953 (C–H aliphatic), 1695 (C=O), 1571 (C=N), 1237 (C–N) and 841 (C–Cl); $^1\text{H-NMR}$ (DMSO- d_6 , 300 MHz): δ (ppm) 2.51 (4H; t; $\text{CH}_2\text{-N}$; b + b'), 3.30 (4H; t; $\text{CH}_2\text{-N}$; a + a'), 5.06 (2H; s; $-\text{N-CH}_2\text{-C=O}$), 6.94 (1H; d; pyridazinone H^5), 6.98 (1H; d; pyridazinone H^4), 7.01–7.70 (7H; m; phenyl protons), 7.99 (1H; s; $-\text{N=CH-}$) and 11.74 (1H; s; $-\text{NH-N}$); $^{13}\text{C-NMR}$ (DMSO- d_6 , 300 MHz), δ 46.23 (2C; $\text{CH}_2\text{-N}$), 47.56 (2C; $\text{CH}_2\text{-N}$), 79.01 (1C; $-\text{N-CH}_2\text{-C=O}$), 114.27 (1C; =CH), 116.21 (1C; pyridazinone C^5), 117.02 (1C; 3,4-dichlorophenyl C^6), 120.34 (1C; 3,4-dichlorophenyl C^5), 127.07 (1C; pyridazinone C^4), 130.56 (2C; 4-bromophenyl $\text{C}^{2,6}$), 130.72 (2C; 4-bromophenyl $\text{C}^{3,5}$), 130.90 (1C; 3,4-dichlorophenyl C^2), 132.03 (1C; phenyl C^1), 144.36 (1C; 3,4-dichlorophenyl C^1), 146.96 (1C; pyridazinone C^6), 148.56 (1C; 4-bromophenyl C^4), 150.93 (2C; 3,4-dichlorophenyl $\text{C}^{3,4}$), 158.07 (1C; $\text{CH}_2\text{-N-C=O}$) and 165.70 (1C; pyridazinone C^3); $\text{C}_{23}\text{H}_{21}\text{BrCl}_2\text{N}_6\text{O}_2$ MS (ESI+) calculated: 564.03, Found: *m/e* 565.0342 (M^+ ; 100.0%), 567.0299 (M^{+2} ; 45.7%) and 568.0392 (M^{+4} ; 6.2%).

6-(4-(3,4-Dichlorophenyl)piperazine-1-yl)-3(2H)-pyridazinone-2-acetyl-2-(2-chlorobenzal)hydrazon (**5c**)

White crystals; yield: 81.24%; mp: 267–269 °C; IR (ν cm^{-1} , ATR): 3063 (C–H aromatic), 2952 (C–H aliphatic), 1695 (C=O), 1569 (C=N), 1237 (C–N) and 839 (C–Cl); $^1\text{H-NMR}$ (DMSO- d_6 , 300 MHz): δ (ppm) 3.12 (4H; t; $\text{CH}_2\text{-N}$; b + b'), 3.30 (4H; t; $\text{CH}_2\text{-N}$; a + a'), 5.12 (2H; s; $-\text{N-CH}_2\text{-C=O}$), 6.66 (1H; d; pyridazinone H^5), 6.88 (1H; d; pyridazinone H^4), 7.10–7.47 (7H; m; phenyl protons), 7.80 (1H; s; $-\text{N=CH-}$) and 11.12 (1H; s; $-\text{NH-N}$); $^{13}\text{C-NMR}$ (DMSO- d_6 , 300 MHz), δ 46.61 (2C; $\text{CH}_2\text{-N}$), 48.32 (2C; $\text{CH}_2\text{-N}$), 77.12 (1C; $-\text{N-CH}_2\text{-C=O}$), 115.87 (1C; =CH), 116.85 (1C; pyridazinone C^5), 117.21 (1C; 3,4-dichlorophenyl C^6), 120.55 (1C; 3,4-dichlorophenyl C^5), 126.47 (1C; pyridazinone C^4), 130.23 (1C; 2-chlorophenyl C^4), 130.56 (1C; 2-chlorophenyl C^5), 130.62 (1C; 2-chlorophenyl C^3), 130.74 (1C; 2-chlorophenyl C^6), 131.90 (1C; 3,4-dichlorophenyl C^2), 135.12 (1C; 2-chlorophenyl C^1), 144.36 (1C; 3,4-dichlorophenyl C^1), 146.96 (1C; pyridazinone C^6), 148.56 (1C; 2-chlorophenyl C^2), 150.93 (2C; 3,4-dichlorophenyl $\text{C}^{3,4}$), 158.07 (1C; $\text{CH}_2\text{-N-C=O}$) and 165.70 (1C; pyridazinone C^3); $\text{C}_{23}\text{H}_{21}\text{Cl}_3\text{N}_6\text{O}_2$ MS (ESI+) calculated: 518.08, Found: *m/e* 519.0864 (M^+ ;

100.0%), 523.0827 (M^{+4} ; 30.7%) and 524.0864 (M^{+6} ; 3.4%).

6-(4-(3,4-Dichlorophenyl)piperazine-1-yl)-3(2H)-pyridazinone-2-acetyl-2-(4-chlorobenzal)hydrazon (**5d**)

White crystals; yield: 56.24%; mp: 275–277 °C; IR (ν cm^{-1} , ATR): 3066 (C–H aromatic), 2919 (C–H aliphatic), 1667 (C=O), 1596 (C=N), 1238 (C–N) and 837 (C–Cl); $^1\text{H-NMR}$ (CDCl_3 - d , 300 MHz): δ (ppm) 3.31 (4H; t; $\text{CH}_2\text{-N}$; b + b'), 3.50 (4H; t; $\text{CH}_2\text{-N}$; a + a'), 5.28 (2H; s; $-\text{N-CH}_2\text{-C=O}$), 6.90 (1H; d; pyridazinone H^5), 6.98 (1H; d; pyridazinone H^4), 7.02–7.44 (7H; m; phenyl protons), 8.18 (1H; s; $-\text{N=CH-}$) and 10.51 (1H; s; $-\text{NH-N}$); $^{13}\text{C-NMR}$ (DMSO- d_6 , 300 MHz), δ 46.17 (2C; $\text{CH}_2\text{-N}$), 47.59 (2C; $\text{CH}_2\text{-N}$), 79.14 (1C; $-\text{N-CH}_2\text{-C=O}$), 112.20 (1C; =CH), 116.08 (1C; pyridazinone C^5), 117.03 (1C; 3,4-dichlorophenyl C^6), 120.52 (1C; 3,4-dichlorophenyl C^5), 128.97 (1C; pyridazinone C^4), 130.92 (2C; 4-chlorophenyl $\text{C}^{2,6}$), 131.90 (2C; 4-chlorophenyl $\text{C}^{3,5}$), 134.88 (1C; 3,4-dichlorophenyl C^2), 139.99 (1C; 4-chlorophenyl C^1), 143.10 (1C; 3,4-dichlorophenyl C^1), 146.21 (1C; pyridazinone C^6), 148.98 (1C; 4-chlorophenyl C^4), 150.99 (2C; 3,4-dichlorophenyl $\text{C}^{3,4}$), 158.31 (1C; $\text{CH}_2\text{-N-C=O}$) and 168.49 (1C; pyridazinone C^3); $\text{C}_{23}\text{H}_{21}\text{Cl}_3\text{N}_6\text{O}_2$ MS (ESI+) calculated: 518.08, Found: *m/e* 519.0859 (M^+ ; 100.0%), 523.0807 (M^{+4} ; 30.7%) and 524.0828 (M^{+6} ; 3.4%).

6-[4-(3,4-Dichlorophenyl)piperazine-1-yl]-3(2H)-pyridazinone-2-acetyl-2-(4-fluorobenzal)hydrazon (**5e**)

White crystals; yield: 84.03%; mp: 228–230 °C; IR (ν cm^{-1} , ATR): 3001 (C–H aromatic), 2972 (C–H aliphatic), 1687 (C=O), 1585 (C=N), 1236 (C–N) and 836 (C–Cl); $^1\text{H-NMR}$ (CDCl_3 - d , 300 MHz): δ (ppm) 3.10 (4H; t; $\text{CH}_2\text{-N}$; b + b'), 3.27 (4H; t; $\text{CH}_2\text{-N}$; a + a'), 5.09 (2H; s; $-\text{N-CH}_2\text{-C=O}$), 6.65 (1H; d; pyridazinone H^5), 6.79 (1H; d; pyridazinone H^4), 6.84–7.53 (7H; m; phenyl protons), 7.78 (1H; s; $-\text{N=CH-}$) and 11.10 (1H; s; $-\text{NH-N}$); $^{13}\text{C-NMR}$ (DMSO- d_6 , 300 MHz), δ 46.17 (2C; $\text{CH}_2\text{-N}$), 47.59 (2C; $\text{CH}_2\text{-N}$), 78.92 (1C; $-\text{N-CH}_2\text{-C=O}$), 116.10 (1C; =CH), 116.17 (1C; pyridazinone C^5), 117.03 (1C; 3,4-dichlorophenyl C^6), 120.50 (1C; 3,4-dichlorophenyl C^5), 127.09 (1C; pyridazinone C^4), 129.60 (2C; 4-fluorophenyl $\text{C}^{2,6}$), 131.00 (2C; 4-fluorophenyl $\text{C}^{3,5}$), 134.88 (1C; 3,4-dichlorophenyl C^2), 143.28 (1C; 4-fluorophenyl C^1), 146.42 (1C; 3,4-dichlorophenyl C^1), 149.01 (1C; pyridazinone C^6), 151.01 (1C; 4-fluorophenyl C^4), 158.34 (2C; 3,4-dichlorophenyl $\text{C}^{3,4}$), 161.86 (1C; $\text{CH}_2\text{-N-C=O}$) and 168.45 (1C; pyridazinone C^3); $\text{C}_{23}\text{H}_{21}\text{Cl}_2\text{FN}_6\text{O}_2$ MS (ESI+) calculated: 502.11, Found: *m/e* 503.1142 (M^+ ; 100.0%), 505.1117 (M^{+2} ; 64.9%) and 507.1105 (M^{+4} ; 10.2%).

6-[4-(3,4-Dichlorophenyl)piperazine-1-yl]-3(2H)-pyridazinone-2-acetyl-2-(3-methylbenzyl)hydrazon (**5f**)

White crystals; yield: 79.28%; mp: 297–299 °C; IR (ν cm⁻¹, ATR): 3059 (C–H aromatic), 2888 (C–H aliphatic), 1693 (C=O), 1570 (C=N), 1237 (C–N) and 845 (C–Cl); ¹H-NMR (DMSO-*d*₆, 300 MHz): δ (ppm) 2.51 (3H; s; –CH₃), 3.29 (4H; t; CH₂–N; b + b'), 3.37 (4H; t; CH₂–N; a + a'), 5.06 (2H; s; –N–CH₂–C=O), 7.32 (1H; d; pyridazinone H⁵), 7.33 (1H; d; pyridazinone H⁴), 7.34–7.66 (7H; m; phenyl protons), 7.98 (1H; s; –N=CH–) and 11.62 (1H; s; –NH–N); ¹³C-NMR (DMSO-*d*₆, 300 MHz), δ 21.35 (1C; –CH₃), 46.17 (2C; CH₂–N), 47.56 (2C; CH₂–N), 56.49 (1C; –N–CH₂–C=O), 116.08 (1C;=CH), 117.04 (1C; pyridazinone C⁵), 120.42 (1C; 3,4-dichlorophenyl C⁶), 124.75 (1C; 3,4-dichlorophenyl C⁵), 127.67 (1C; pyridazinone C⁴), 129.17 (1C; 3-methylphenyl C²), 130.95 (1C; 3-methylphenyl C⁴), 131.99 (1C; 3-methylphenyl C⁵), 134.38 (1C; 3-methylphenyl C⁶), 138.54 (1C; 3-methylphenyl C³), 144.42 (1C; 3,4-dichlorophenyl C²), 147.47 (1C; 3-methylphenyl C¹), 148.92 (1C; 3,4-dichlorophenyl C¹), 151.04 (1C; pyridazinone C⁶), 158.23 (2C; 3,4-dichlorophenyl C^{3,4}), 163.71 (1C; CH₂–N–C=O) and 168.42 (1C; pyridazinone C³); C₂₄H₂₄Cl₂N₆O₂ MS (ESI+) calculated: 498.13, Found: *m/e* 499.1408 (M⁺; 100.0%), 501.1368 (M⁺²; 64.5%) and 502.1409 (M⁺⁴; 10.6%).

6-[4-(3,4-Dichlorophenyl)piperazine-1-yl]-3(2H)-pyridazinone-2-acetyl-2-(4-methylbenzyl)hydrazon (**5g**)

White crystals; yield: 81.79%; mp: 255–257 °C; IR (ν cm⁻¹, ATR): 3086 (C–H aromatic), 2953 (C–H aliphatic), 1684 (C=O), 1568 (C=N), 1237 (C–N) and 840 (C–Cl); ¹H-NMR (CDCl₃-*d*, 300 MHz): δ (ppm) 2.24 (3H; s; –CH₃), 3.12 (4H; t; CH₂–N; b + b'), 3.29 (4H; t; CH₂–N; a + a'), 5.11 (2H; s; –N–CH₂–C=O), 6.65 (1H; d; pyridazinone H⁵), 6.68 (1H; d; pyridazinone H⁴), 6.78–7.43 (7H; m; phenyl protons), 7.78 (1H; s; –N=CH–) and 10.89 (1H; s; –NH–N); ¹³C-NMR (DMSO-*d*₆, 300 MHz), δ 28.56 (1C; –CH₃), 47.21 (2C; CH₂–N), 48.32 (2C; CH₂–N), 78.57 (1C; –N–CH₂–C=O), 114.53 (1C;=CH), 116.03 (1C; pyridazinone C⁵), 118.56 (1C; 3,4-dichlorophenyl C⁶), 121.42 (1C; 3,4-dichlorophenyl C⁵), 130.14 (1C; pyridazinone C⁴), 130.86 (1C; 4-methylphenyl C²), 130.98 (1C; 4-methylphenyl C⁴), 131.90 (1C; 4-methylphenyl C⁵), 132.00 (1C; 4-methylphenyl C⁶), 134.88 (1C; 4-methylphenyl C³), 137.45 (1C; 3,4-dichlorophenyl C²), 138.99 (1C; 4-methylphenyl C¹), 143.10 (1C; 3,4-dichlorophenyl C¹), 146.21 (1C; pyridazinone C⁶), 151.87 (2C; 3,4-dichlorophenyl C^{3,4}), 158.31 (1C; CH₂–N–C=O) and 168.52 (1C; pyridazinone C³); C₂₄H₂₄Cl₂N₆O₂ MS (ESI+) calculated: 498.13, Found: *m/e* 499.1443 (M⁺; 100.0%), 501.1412 (M⁺²; 64.5%) and 503.1402 (M⁺⁴; 10.6%).

6-[4-(3,4-Dichlorophenyl)piperazine-1-yl]-3(2H)-pyridazinone-2-acetyl-2-(2-methoxybenzyl)hydrazon (**5h**)

White crystals; yield: 86.32%; mp: 263–265 °C; IR (ν cm⁻¹, ATR): 3063 (C–H aromatic), 2953 (C–H aliphatic), 1695 (C=O), 1568 (C=N), 1236 (C–N), 1091 (C–O) and 839 (C–Cl); ¹H-NMR (CDCl₃-*d*, 300 MHz): δ (ppm) 3.05 (4H; t; CH₂–N; b + b'), 3.46 (4H; t; CH₂–N; a + a'), 4.87 (3H; s; –O–CH₃), 5.29 (2H; s; –N–CH₂–C=O), 6.82 (1H; d; pyridazinone H⁵), 6.86 (1H; d; pyridazinone H⁴), 6.94–7.84 (7H; m; phenyl protons), 8.06 (1H; s; –N=CH–) and 10.59 (1H; s; –NH–N); ¹³C-NMR (DMSO-*d*₆, 300 MHz), δ 46.61 (2C; CH₂–N), 48.32 (2C; CH₂–N), 56.01 (1C; O–CH₃), 77.12 (1C; –N–CH₂–C=O), 115.87 (1C;=CH), 116.03 (1C; pyridazinone C⁵), 117.21 (1C; 3,4-dichlorophenyl C⁶), 120.55 (1C; 3,4-dichlorophenyl C⁵), 126.47 (1C; pyridazinone C⁴), 130.23 (1C; 2-methoxyphenyl C⁴), 130.62 (1C; 2-methoxyphenyl C⁵), 130.74 (1C; 2-methoxyphenyl C³), 130.98 (1C; 2-methoxyphenyl C⁶), 131.90 (1C; 3,4-dichlorophenyl C²), 135.12 (1C; 2-methoxyphenyl C¹), 144.36 (1C; 3,4-dichlorophenyl C¹), 146.96 (1C; pyridazinone C⁶), 148.56 (1C; 2-methoxyphenyl C²), 150.93 (2C; 3,4-dichlorophenyl C^{3,4}), 158.07 (1C; CH₂–N–C=O) and 165.70 (1C; pyridazinone C³); C₂₄H₂₄Cl₂N₆O₃ MS (ESI+) calculated: 514.13, Found: *m/e* 515.1364 (M⁺; 100.0%), 517.1365 (M⁺²; 65.1%) and 518.1400 (M⁺⁴; 10.2%).

6-[4-(3,4-Dichlorophenyl)piperazine-1-yl]-3(2H)-pyridazinone-2-acetyl-2-(3-methoxybenzyl)hydrazon (**5i**)

White crystals; yield: 80.32%; mp: 258–260 °C; IR (ν cm⁻¹, ATR): 3080 (C–H aromatic), 2954 (C–H aliphatic), 1695 (C=O), 1569 (C=N), 1236 (C–N), 1042 (C–O) and 844 (C–Cl); ¹H-NMR (DMSO-*d*₆, 300 MHz): δ (ppm) 2.52 (4H; t; CH₂–N; b + b'), 3.81 (4H; t; CH₂–N; a + a'), 4.68 (3H; s; –O–CH₃), 5.08 (2H; s; –N–CH₂–C=O), 6.92 (1H; d; pyridazinone H⁵), 7.02 (1H; d; pyridazinone H⁴), 7.21–7.68 (7H; m; phenyl protons), 7.99 (1H; s; –N=CH–) and 11.68 (1H; s; –NH–N); ¹³C-NMR (DMSO-*d*₆, 300 MHz), δ 46.17 (2C; CH₂–N), 47.21 (2C; CH₂–N), 55.99 (1C; O–CH₃), 78.57 (1C; –N–CH₂–C=O), 113.66 (1C;=CH), 116.03 (1C; pyridazinone C⁵), 117.21 (1C; 3,4-dichlorophenyl C⁶), 120.52 (1C; 3,4-dichlorophenyl C⁵), 129.27 (1C; pyridazinone C⁴), 130.93 (1C; 3-methoxyphenyl C⁴), 130.98 (1C; 3-methoxyphenyl C⁵), 131.90 (1C; 3-methoxyphenyl C²), 132.00 (1C; 3-methoxyphenyl C⁶), 134.88 (1C; 3,4-dichlorophenyl C²), 139.99 (1C; 3-methoxyphenyl C¹), 143.10 (1C; 3,4-dichlorophenyl C¹), 146.21 (1C; pyridazinone C⁶), 148.45 (1C; 3-methoxyphenyl C²), 150.99 (2C; 3,4-dichlorophenyl C^{3,4}), 158.31 (1C; CH₂–N–C=O) and 168.49 (1C; pyridazinone C³); C₂₄H₂₄Cl₂N₆O₃ MS (ESI+) calculated:

514.13, Found: *m/e* 515.1358 (M^+ ; 100.0%), 517.1332 (M^{+2} ; 65.1%) and 518.1354 (M^{+4} ; 10.2%).

6-[4-(3,4-Dichlorophenyl)piperazine-1-yl]-3(2H)-pyridazinone-2-acetyl-2-(4-methoxybenzal)hydrazon (5k)

White crystals; yield: 93.86%; mp: 228–230 °C; IR (ν cm^{-1} , ATR): 3065 (C–H aromatic), 2953 (C–H aliphatic), 1683 (C=O), 1574 (C=N), 1237 (C–N), 1032 (C–O) and 826 (C–Cl); $^1\text{H-NMR}$ (DMSO- d_6 , 300 MHz): δ (ppm) 2.51 (4H; t; $\text{CH}_2\text{-N}$; b + b'), 3.29 (4H; t; $\text{CH}_2\text{-N}$; a + a'), 3.81 (3H; s; $-\text{O}-\text{CH}_3$), 5.04 (2H; s; $-\text{N}-\text{CH}_2\text{-C}=\text{O}$), 6.92 (1H; d; pyridazinone H^5), 6.98 (1H; d; pyridazinone H^4), 7.01–7.67 (7H; m; phenyl protons), 7.96 (1H; s; $-\text{N}=\text{CH}-$) and 11.53 (1H; s; $-\text{NH}-\text{N}$); $^{13}\text{C-NMR}$ (DMSO- d_6 , 300 MHz), δ 46.17 (2C; $\text{CH}_2\text{-N}$), 47.59 (2C; $\text{CH}_2\text{-N}$), 53.07 (1C; $\text{O}-\text{CH}_3$), 79.14 (1C; $-\text{N}-\text{CH}_2\text{-C}=\text{O}$), 112.20 (1C; =CH), 117.03 (1C; pyridazinone C^5), 117.21 (1C; 3,4-dichlorophenyl C^6), 120.52 (1C; 3,4-dichlorophenyl C^5), 128.97 (1C; pyridazinone C^4), 130.92 (2C; 4-methoxyphenyl $\text{C}^{2,6}$), 132.00 (2C; 4-methoxyphenyl $\text{C}^{3,5}$), 134.88 (1C; 3,4-dichlorophenyl C^2), 139.99 (1C; 4-methoxyphenyl C^1), 143.10 (1C; 3,4-dichlorophenyl C^1), 146.21 (1C; pyridazinone C^6), 148.98 (1C; 4-methoxyphenyl C^4), 150.99 (2C; 3,4-dichlorophenyl $\text{C}^{3,4}$), 158.31 (1C; $\text{CH}_2\text{-N}-\text{C}=\text{O}$) and 168.49 (1C; pyridazinone C^3); $\text{C}_{24}\text{H}_{24}\text{Cl}_2\text{N}_6\text{O}_3$ MS (ESI+) calculated: 514.13, Found: *m/e* 515.1380 (M^+ ; 100.0%), 517.1362 (M^{+2} ; 65.1%) and 518.1405 (M^{+4} ; 10.2%).

6-[4-(3,4-Dichlorophenyl)piperazine-1-yl]-3(2H)-pyridazinone-2-acetyl-2-(2,3-dimethoxybenzal)hydrazon (5l)

White crystals; yield: 75.12%; mp: 265–267 °C; IR (ν cm^{-1} , ATR): 3040 (C–H aromatic), 2969 (C–H aliphatic), 1690 (C=O), 1592 (C=N), 1231 (C–N), 1065 (C–O) and 836 (C–Cl); $^1\text{H-NMR}$ (DMSO- d_6 , 300 MHz): δ (ppm) 3.27 (4H; t; $\text{CH}_2\text{-N}$; b + b'), 3.54 (4H; t; $\text{CH}_2\text{-N}$; a + a'), 3.76 (3H; s; $-\text{O}-\text{CH}_3$), 3.82 (3H; s; $-\text{O}-\text{CH}_3$), 5.04 (2H; s; $-\text{N}-\text{CH}_2\text{-C}=\text{O}$), 6.98 (1H; d; pyridazinone H^5), 7.10 (1H; d; pyridazinone H^4), 7.11–7.62 (6H; m; phenyl protons), 8.28 (1H; s; $-\text{N}=\text{CH}-$) and 11.59 (1H; s; $-\text{NH}-\text{N}$); $^{13}\text{C-NMR}$ (DMSO- d_6 , 300 MHz), δ 46.12 (2C; $\text{CH}_2\text{-N}$), 47.56 (2C; $\text{CH}_2\text{-N}$), 56.21 (1C; $\text{O}-\text{CH}_3$), 56.56 (1C; $\text{O}-\text{CH}_3$), 61.70 (1C; $-\text{N}-\text{CH}_2\text{-C}=\text{O}$), 114.65 (1C; =CH), 116.14 (1C; pyridazinone C^5), 117.02 (1C; 3,4-dichlorophenyl C^6), 117.41 (1C; 3,4-dichlorophenyl C^5), 120.48 (1C; pyridazinone C^4), 124.94 (1C; 2,3-dimethoxyphenyl C^5), 127.78 (1C; 2,3-dimethoxyphenyl C^6), 130.99 (1C; 2,3-dimethoxyphenyl C^4), 131.98 (1C; 3,4-dichlorophenyl C^2), 140.30 (2C; 3,4-dichlorophenyl C^1), 2,3-dimethoxyphenyl C^1), 148.33 (1C; pyridazinone C^6), 149.09 (2C; 2,3-

dimethoxyphenyl $\text{C}^{2,3}$), 151.01 (2C; 3,4-dichlorophenyl $\text{C}^{3,4}$), 153.10 (1C; $\text{CH}_2\text{-N}-\text{C}=\text{O}$) and 158.44 (1C; pyridazinone C^3); $\text{C}_{25}\text{H}_{26}\text{Cl}_2\text{N}_6\text{O}_4$ MS (ESI+) calculated: 544.14, Found: *m/e* 545.1468 (M^+ ; 100.0%), 547.1440 (M^{+2} ; 65.4%) and 548.1469 (M^{+4} ; 10.2%).

6-[4-(3,4-Dichlorophenyl)piperazine-1-yl]-3(2H)-pyridazinone-2-acetyl-2-(3,5-dimethoxybenzal)hydrazon (5m)

White crystals; yield: 65.27%; mp: 271–273 °C; IR (ν cm^{-1} , ATR): 3040 (C–H aromatic), 2960 (C–H aliphatic), 1681 (C=O), 1578 (C=N), 1235 (C–N), 1064 (C–O) and 827 (C–Cl); $^1\text{H-NMR}$ (DMSO- d_6 , 300 MHz): δ (ppm) 3.27 (4H; t; $\text{CH}_2\text{-N}$; b + b'), 3.38 (4H; t; $\text{CH}_2\text{-N}$; a + a'), 3.78 (6H; s; $-\text{O}-\text{CH}_3$), 5.06 (2H; s; $-\text{N}-\text{CH}_2\text{-C}=\text{O}$), 6.86 (1H; d; pyridazinone H^5), 6.91 (1H; d; pyridazinone H^4), 6.93–7.90 (6H; m; phenyl protons), 8.19 (1H; s; $-\text{N}=\text{CH}-$) and 11.62 (1H; s; $-\text{NH}-\text{N}$); $^{13}\text{C-NMR}$ (DMSO- d_6 , 300 MHz), δ 46.27 (2C; $\text{CH}_2\text{-N}$), 47.75 (2C; $\text{CH}_2\text{-N}$), 55.63 (2C; $\text{O}-\text{CH}_3$), 79.14 (1C; $-\text{N}-\text{CH}_2\text{-C}=\text{O}$), 102.53 (1C; =CH), 104.97 (1C; pyridazinone C^5), 105.27 (1C; 3,4-dichlorophenyl C^6), 120.52 (1C; 3,4-dichlorophenyl C^5), 126.89 (1C; pyridazinone C^4), 130.76 (2C; 3,5-dimethoxyphenyl $\text{C}^{2,6}$), 130.93 (1C; 3,4-dichlorophenyl C^2), 132.12 (1C; 3,5-dimethoxyphenyl C^4), 136.37 (1C; 3,5-dimethoxyphenyl C^1), 144.06 (1C; 3,4-dichlorophenyl C^1), 148.84 (1C; pyridazinone C^6), 150.89 (2C; 3,5-dimethoxyphenyl $\text{C}^{3,5}$), 158.25 (2C; 3,4-dichlorophenyl $\text{C}^{3,4}$), 161.06 (1C; $\text{CH}_2\text{-N}-\text{C}=\text{O}$) and 168.38 (1C; pyridazinone C^3); $\text{C}_{25}\text{H}_{26}\text{Cl}_2\text{N}_6\text{O}_4$ MS (ESI+) calculated: 544.14, Found: *m/e* 545.1475 (M^+ ; 100.0%), 547.1434 (M^{+2} ; 65.4%) and 548.1468 (M^{+4} ; 10.2%).

6-[4-(3,4-Dichlorophenyl)piperazine-1-yl]-3(2H)-pyridazinone-2-acetyl-2-(2,4,6-trimethoxybenzal)hydrazon (5n)

White crystals; yield: 61.86%; mp: 273–275 °C; IR (ν cm^{-1} , ATR): 3083 (C–H aromatic), 2969 (C–H aliphatic), 1667 (C=O), 1592 (C=N), 1238 (C–N), 1061 (C–O) and 836 (C–Cl); $^1\text{H-NMR}$ (DMSO- d_6 , 300 MHz): δ (ppm) 3.30 (4H; t; $\text{CH}_2\text{-N}$; b + b'), 3.56 (4H; t; $\text{CH}_2\text{-N}$; a + a'), 3.79 (3H; s; $-\text{O}-\text{CH}_3$), 3.82 (6H; s; $-\text{O}-\text{CH}_3$), 4.94 (2H; s; $-\text{N}-\text{CH}_2\text{-C}=\text{O}$), 6.27 (1H; d; pyridazinone H^5), 6.28 (1H; d; pyridazinone H^4), 6.89–7.65 (5H; m; phenyl protons), 8.19 (1H; s; $-\text{N}=\text{CH}-$) and 11.27 (1H; s; $-\text{NH}-\text{N}$); $^{13}\text{C-NMR}$ (DMSO- d_6 , 300 MHz), δ 46.17 (2C; $\text{CH}_2\text{-N}$), 47.59 (2C; $\text{CH}_2\text{-N}$), 55.04 (3C; $\text{O}-\text{CH}_3$), 79.14 (1C; $-\text{N}-\text{CH}_2\text{-C}=\text{O}$), 112.20 (1C; =CH), 115.45 (1C; pyridazinone C^5), 117.03 (1C; 3,4-dichlorophenyl C^6), 120.52 (1C; 3,4-dichlorophenyl C^5), 128.97 (1C; pyridazinone C^4), 131.90 (1C; 3,4-dichlorophenyl C^2), 134.88 (2C; 2,4,6-

trimethoxyphenyl C^{3,5}), 139.99 (1C; 2,4,6-trimethoxyphenyl C¹), 143.10 (1C; 3,4-dichlorophenyl C¹), 146.21 (1C; pyridazinone C⁶), 148.98 (1C; 2,4,6-trimethoxyphenyl C⁴), 149.07 (2C; 2,4,6-trimethoxyphenyl C^{2,6}), 150.99 (2C; 3,4-dichlorophenyl C^{3,4}), 158.31 (1C; CH₂-N-C=O) and 168.49 (1C; pyridazinone C³). C₂₆H₂₈Cl₂N₆O₅ MS (ESI+) calculated: 574.15, Found: *m/e* 575.1569 (M⁺; 100.0%), 577.1545 (M⁺²; 65.6%) and 579.1544 (M⁺⁴; 10.2%).

6-[4-(3,4-Dichlorophenyl)piperazine-1-yl]-3(2H)-pyridazinone-2-acetyl-2-(3,4,5-trimethoxybenzal)hydrazon (5o)

White crystals; yield: 67.02%; mp: 286–288 °C; IR (ν cm⁻¹, ATR): 3080 (C–H aromatic), 2938 (C–H aliphatic), 1662 (C=O), 1591 (C=N), 1234 (C–N), 1078 (C–O) and 826 (C–Cl); ¹H-NMR (DMSO-*d*₆, 300 MHz): δ (ppm) 3.28 (4H; t; CH₂-N; b + b'), 3.36 (4H; t; CH₂-N; a + a'), 3.70 (3H; s; -O-CH₃), 3.83 (6H; s; -O-CH₃), 5.07 (2H; s; -N-CH₂-C=O), 6.99 (1H; d; pyridazinone H⁵), 7.01 (1H; d; pyridazinone H⁴), 7.02–7.66 (5H; m; phenyl protons), 7.92 (1H; s; -N=CH-) and 11.66 (1H; s; -NH-N); ¹³C-NMR (DMSO-*d*₆, 300 MHz), δ 46.20 (2C; CH₂-N), 47.55 (2C; CH₂-N), 56.40 (3C; O-CH₃), 60.57 (1C; -N-CH₂-C=O), 104.79 (1C;=CH), 116.09 (1C; pyridazinone C⁵), 117.04 (1C; 3,4-dichlorophenyl C⁶), 120.43 (1C; 3,4-dichlorophenyl C⁵), 127.18 (1C; pyridazinone C⁴), 130.10 (1C; 3,4-dichlorophenyl C²), 139.51 (2C; 3,4,5-trimethoxyphenyl C^{2,6}), 139.68 (1C; 3,4,5-trimethoxyphenyl C¹), 144.07 (1C; 3,4-dichlorophenyl C¹), 147.39 (1C; pyridazinone C⁶), 153.63 (3C; 3,4,5-trimethoxyphenyl C^{3,4,5}), 158.21 (2C; 3,4-dichlorophenyl C^{3,4}), 163.69 (1C; CH₂-N-C=O) and 168.46 (1C; pyridazinone C³); C₂₆H₂₈Cl₂N₆O₅ MS (ESI+) calculated: 574.15, Found: *m/e* 575.1580 (M⁺; 100.0%), 577.1530 (M⁺²; 65.6%) and 578.1566 (M⁺⁴; 10.2%).

6-[4-(3,4-Dichlorophenyl)piperazine-1-yl]-3(2H)-pyridazinone-2-acetyl-2-(4-dimethylaminobenzal)hydrazon (5p)

Pale-yellow crystals; yield: 78.30%; mp: 284–286 °C; IR (ν cm⁻¹, ATR): 3091 (C–H aromatic), 2972 (C–H aliphatic), 1660 (C=O), 1590 (C=N), 1235 (C–N) and 843 (C–Cl); ¹H-NMR (DMSO-*d*₆, 300 MHz): δ (ppm) 2.97 (6H; s; N-(CH₃)₂), 3.29 (4H; t; CH₂-N; b + b'), 3.31 (4H; t; CH₂-N; a + a'), 5.01 (2H; s; -N-CH₂-C=O), 6.72 (1H; d; pyridazinone H⁵), 6.90 (1H; d; pyridazinone H⁴), 6.98–7.66 (7H; m; phenyl protons), 7.88 (1H; s; -N=CH-) and 11.36 (1H; s; -NH-N); ¹³C-NMR (DMSO-*d*₆, 300 MHz), δ 42.35 (2C; N-(CH₃)₂), 46.17 (2C; CH₂-N), 47.59 (2C; CH₂-N), 79.14 (1C; -N-CH₂-C=O), 112.20 (1C;=CH), 116.09 (1C; pyridazinone C⁵), 117.03 (1C; 3,4-dichlorophenyl C⁶),

120.52 (1C; 3,4-dichlorophenyl C⁵), 128.97 (1C; pyridazinone C⁴), 130.92 (2C; 4-dimethylaminophenyl C^{2,6}), 132.00 (2C; 4-dimethylaminophenyl C^{3,5}), 134.88 (1C; 3,4-dichlorophenyl C²), 139.99 (1C; 4-dimethylaminophenyl C¹), 143.10 (1C; 4-dimethylaminophenyl C⁴), 146.21 (1C; 3,4-dichlorophenyl C¹), 148.98 (1C; pyridazinone C⁶), 150.99 (2C; 3,4-dichlorophenyl C^{3,4}), 158.31 (1C; CH₂-N-C=O) and 168.46 (1C; pyridazinone C³); C₂₅H₂₇Cl₂N₇O₂ MS (ESI+) calculated: 527.16, Found: *m/e* 528.1679 (M⁺; 100.0%), 530.1692 (M⁺²; 65.0%) and 532.1642 (M⁺⁴; 10.2%).

6-[4-(3,4-Dichlorophenyl)piperazine-1-yl]-3(2H)-pyridazinone-2-acetyl-2-(4-nitrobenzal)hydrazon (5r)

Yellow crystals; yield: 85.27%; mp: 207–209 °C; IR (ν cm⁻¹, ATR): 3074 (C–H aromatic), 2842 (C–H aliphatic), 1691 (C=O), 1579 (C=N), 1234 (C–N), 926 (N–O) and 833 (C–Cl); ¹H-NMR (DMSO-*d*₆, 300 MHz): δ (ppm) 3.29 (4H; t; CH₂-N; b + b'), 3.37 (4H; t; CH₂-N; a + a'), 5.11 (2H; s; -N-CH₂-C=O), 6.92 (1H; d; pyridazinone H⁵), 6.98 (1H; d; pyridazinone H⁴), 7.00–7.97 (7H; m; phenyl protons), 8.12 (1H; s; -N=CH-) and 11.98 (1H; s; -NH-N); ¹³C-NMR (DMSO-*d*₆, 300 MHz), δ 46.13 (2C; CH₂-N), 48.59 (2C; CH₂-N), 78.14 (1C; -N-CH₂-C=O), 114.03 (1C;=CH), 116.09 (1C; pyridazinone C⁵), 118.13 (1C; 3,4-dichlorophenyl C⁶), 121.52 (1C; 3,4-dichlorophenyl C⁵), 128.63 (1C; pyridazinone C⁴), 131.92 (1C; 4-nitrophenyl C²), 132.01 (1C; 4-nitrophenyl C⁶), 132.90 (1C; 4-nitrophenyl C³), 133.00 (1C; 4-nitrophenyl C⁵), 134.88 (1C; 3,4-dichlorophenyl C²), 140.07 (1C; 4-nitrophenyl C¹), 143.10 (1C; 4-nitrophenyl C⁴), 147.21 (1C; 3,4-dichlorophenyl C¹), 148.98 (1C; pyridazinone C⁶), 150.99 (2C; 3,4-dichlorophenyl C^{3,4}), 158.31 (1C; CH₂-N-C=O) and 168.49 (1C; pyridazinone C³); C₂₃H₂₁Cl₂N₇O₄ MS (ESI+) calculated: 529.10, Found: *m/e* 530.1080 (M⁺; 100.0%), 532.1066 (M⁺²; 64.6%) and 534.1066 (M⁺⁴; 11.2%).

6-[4-(3,4-Dichlorophenyl)piperazine-1-yl]-3(2H)-pyridazinone-2-acetyl-2-(2-cyanobenzal)hydrazon (5s)

White crystals; yield: 88.73%; mp: 236–8 °C; IR (ν cm⁻¹, ATR): 3068 (C–H aromatic), 2968 (C–H aliphatic), 2227 (C≡N), 1687 (C=O), 1567 (C=N), 1238 (C–N) and 844 (C–Cl); ¹H-NMR (DMSO-*d*₆, 300 MHz): δ (ppm) 3.29 (4H; t; CH₂-N; b + b'), 3.37 (4H; t; CH₂-N; a + a'), 5.09 (2H; s; -N-CH₂-C=O), 7.41 (1H; d; pyridazinone H⁵), 7.42 (1H; d; pyridazinone H⁴), 7.59–7.99 (7H; m; phenyl protons), 8.26 (1H; s; -N=CH-) and 11.95 (1H; s; -NH-N); ¹³C-NMR (DMSO-*d*₆, 300 MHz), δ 46.17 (2C; CH₂-N), 47.56 (2C; CH₂-N), 53.22 (1C; C≡N), 56.49 (1C; -N-CH₂-C=O), 111.34 (1C;=CH), 118.09 (1C; pyridazinone

C⁵), 120.42 (1C; 3,4-dichlorophenyl C⁶), 127.25 (1C; 3,4-dichlorophenyl C⁵), 128.37 (1C; pyridazinone C⁴), 130.95 (1C; 2-cyanophenyl C⁴), 131.99 (1C; 2-cyanophenyl C⁵), 134.03 (1C; 2-cyanophenyl C³), 136.58 (1C; 2-cyanophenyl C⁶), 137.18 (1C; 3,4-dichlorophenyl C²), 140.40 (1C; 2-cyanophenyl C¹), 142.83 (1C; 2-cyanophenyl C²), 149.01 (1C; 3,4-dichlorophenyl C¹), 151.03 (1C; pyridazinone C⁶), 158.25 (2C; 3,4-dichlorophenyl C^{3,4}), 164.16 (1C; CH₂-N-C=O) and 168.92 (1C; pyridazinone C³); C₂₄H₂₁Cl₂N₇O₂ MS (ESI+) calculated: 509.11, Found: *m/e* 510.1203 (M⁺; 100.0%), 512.1187 (M⁺²; 64.6%) and 513.1224 (M⁺⁴; 10.9%).

6-[4-(3,4-Dichlorophenyl)piperazine-1-yl]-3(2H)-pyridazinone-2-acetyl-2-(3-cyanobenzal)hydrazon (5t)

White crystals; yield: 65.03%; mp: 273–275 °C; IR (ν cm⁻¹, ATR): 3093 (C–H aromatic), 2954 (C–H aliphatic), 2230 (C≡N), 1698 (C=O), 1568 (C=N), 1237 (C–N) and 841 (C–Cl); ¹H-NMR (DMSO-*d*₆, 300 MHz): δ (ppm) 3.28 (4H; t; CH₂-N; b + b'), 3.39 (4H; t; CH₂-N; a + a'), 5.12 (2H; s; -N-CH₂-C=O), 6.88 (1H; d; pyridazinone H⁵), 6.92 (1H; d; pyridazinone H⁴), 7.11–8.05 (7H; m; phenyl protons), 8.18 (1H; s; -N=CH-) and 11.80 (1H; s; -NH-N); ¹³C-NMR (DMSO-*d*₆, 300 MHz), δ 46.27 (2C; CH₂-N), 47.78 (2C; CH₂-N), 53.08 (1C; C≡N), 79.20 (1C; -N-CH₂-C=O), 112.66 (1C;=CH), 115.96 (1C; pyridazinone C⁵), 117.11 (1C; 3,4-dichlorophenyl C⁶), 120.94 (1C; 3,4-dichlorophenyl C⁵), 126.88 (1C; pyridazinone C⁴), 130.18 (1C; 3-cyanophenyl C²), 130.74 (1C; 3-cyanophenyl C⁴), 130.91 (1C; 3-cyanophenyl C⁵), 131.48 (1C; 3-cyanophenyl C⁶), 132.14 (1C; 3,4-dichlorophenyl C²), 133.17 (1C; 3-cyanophenyl C¹), 135.81 (1C; 3-cyanophenyl C³), 141.91 (1C; 3,4-dichlorophenyl C¹), 148.85 (1C; pyridazinone C⁶), 150.85 (2C; 3,4-dichlorophenyl C^{3,4}), 158.27 (1C; CH₂-N-C=O) and 168.61 (1C; pyridazinone C³); C₂₄H₂₁Cl₂N₇O₂ MS (ESI+) calculated: 509.11, Found: *m/e* 510.1224 (M⁺; 100.0%), 512.1208 (M⁺²; 64.6%) and 513.1225 (M⁺⁴; 10.9%).

Anticholinesterase activity

The in vitro inhibition of AChE and BChE for **5a–t** was determined by the method of Ellman et al. (1961) using galantamine (CAS 357-70-0) as reference. Electric eel AChE (Type-VI-S, EC 3.1.1.7, Sigma, St. Louis, MO, USA) and horse serum BChE (EC 3.1.1.8, Sigma) were employed as the enzyme sources, acetylthiocholine iodide and butyrylthiocholine chloride (Sigma) as substrates, and 5,5'-dithio-bis(2-nitrobenzoic)acid (DTNB) for activity determination. All reagents and conditions were the same as previously described (Orhan et al. 2008). Briefly, in this method, 140 μ l 0.1 mM sodium phosphate buffer (pH8.0),

20 μ l DTNB, 20 μ l test solution and 20 μ l AChE/BChE solution were added by multichannel automatic pipette (Gilson pipetman, Middleton, USA) in a 96-well microplate and incubated for 15 min at 25 °C. The reaction was then initiated with the addition of 10 μ l of acetylthiocholine iodide/butyrylthiocholine chloride. The hydrolysis of acetylthiocholine iodide/butyrylthiocholine chloride was determined by the formation of yellow 5-thio-2-nitrobenzoate anion as a result of the reaction of DTNB with thiocholines, catalyzed by enzymes at a wavelength of 412 nm and monitored by a 96-well microplate reader (VersaMax Molecular Devices, North Carolina, USA). The measurements and calculations were evaluated by using Softmax PRO 4.3.2.LS software (Softmax Molecular Devices, Downingtown, USA). The percentage of inhibition of AChE/BChE was determined by comparison of the reaction rates of the samples relative to the blank sample (ethanol in phosphate buffer, pH = 8) using the formula (*E-S*)/*E* × 100, where *E* is the activity of enzyme without test sample and *S* is the activity of enzyme with test sample. The experiments were done in triplicate and the results were expressed as average values with SD.

Molecular docking

Ligands were sketched, their pKa calculations were performed on MarvinSketch, Marvin 15.5.25.0, 2015, ChemAxon (<http://www.chemaxon.com>), and they were prepared for docking using LigPrep, version 3.6, Schrödinger, LLC, New York, NY, 2015. OPLS 2005 force field parameters were used for their minimization (Banks et al. 2005). PDB entries were retrieved from Protein Data Bank (<http://www.rcsb.org/>). Coordinates of the centre of the co-crystallised ligands were picked as the centre of search space for each enzyme and the explicit water molecules in the active site gorges were kept. Molecular docking simulations were performed on Glide, version 6.9, Schrödinger, LLC, New York, NY, 2015 (Friesner et al. 2004, 2006; Halgren et al. 2004) using the following settings: Standard precision with enhanced conformer sampling was set, ligands were kept flexible, 10 poses were written at most per ligand, post-minimization was enabled, and per-residue interaction scores for residues within 12 Å of grid centres were written. Prior to ligand docking, in order to validate our method, we re-docked the co-crystallised ligands, donepezil (PDB ligand code E20) and tacrine (PDB ligand code THA), in AChE and BChE active sites, respectively and were able to reproduce conformers close to the original binding modes (RMSD: 0.82 Å for 4EY7 and 0.85 Å for 4BDS). Docking poses were visually inspected using pose viewer of Maestro, version 10.4, Schrödinger, LLC, New York, NY, 2015.

Acknowledgements This study was funded by the Research Foundation of İnönü University (2013/94).

Compliance with ethical standards

Conflict of interest The authors declare that they have no competing interests.

References

- Abd El-Ghaffar NF, Mohamed MK, Kadah MS, Radwan AM, Said GH, Abd el Al SN (2011) Synthesis and anti-tumor activities of some new pyridazinones containing the 2-phenyl-1*H*-indolyl moiety. *J Chem Pharm Res* 3:248–259
- Anand P, Singh P (2013) A review on cholinesterase inhibitors for Alzheimer's disease. *Arch Pharm Res* 36:375–399
- Ballard C, Gauthier S, Corbett A, Brayne C, Aarsland D, Jones E (2011) Alzheimer's disease. *The Lancet* 377:1019–1031
- Banks JL, Beard HS, Cao Y, Cho AE, Damm W, Farid R, Felts AK, Halgren TA, Mainz DT, Maple JR (2005) Maple, Integrated modeling program, applied chemical theory (IMPACT). *J Comput Chem* 26:1752–1780
- Belluti F, Bartolini M, Bottegoni G, Bisi A, Cavalli A, Andrisano V, Rampa A (2011) Benzophenone-based derivatives: a novel series of potent and selective dual inhibitors of acetylcholinesterase and acetylcholinesterase-induced betaamyloid aggregation. *Eur J Med Chem* 46:1682–1693
- Bentley P, Drive J, Dolan RJ (2011) Cholinergic modulation of cognition: insights from human pharmacological functional neuroimaging. *Prog Neurobiol* 94:360–388
- Bourne Y, Taylor P, Radić Z, Marchot P (2003) Structural insights into ligand interactions at the acetylcholinesterase peripheral anionic site. *EMBO J* 22:1–12
- Brus B, Kosak U, Turk S, Pislari A, Coquelle N, Kos J, Stojan J, Colletier JP, Gobec S (2014) Discovery, biological evaluation, and crystal structure of a novel nanomolar selective butyrylcholinesterase inhibitor. *J Med Chem* 57:8167–8179
- Cacabelos R (2008) Pharmacogenomics in Alzheimer's disease. *Mol Biol* 448:213–353
- Camps P, Formosa X, Galdeano C, Gomez T, Munoz-Torrero D, Scarpellini M, Viayna E, Badia A, Clos MV, Camins A, Pallas M, Bartolini M, Mancini F, Andrisano V, Estelrich J, Lizondo M, Bidon-Chanal A, Luque FJ (2008) Novel donepezil-based inhibitors of acetyl- and butyrylcholinesterase and acetylcholinesterase-induced beta-amyloid aggregation. *J Med Chem* 51:3588–3598
- Camps P, Formosa X, Galdeano C, Gomez T, Munoz-Torrero D, Scarpellini M, Viyana E, Badia A, Clos VM, Camins A, Pallas M, Bartolini M, Mancini F, Andrisano V, Estelrich J, Lizondo M, Bidon-Chanal A, Luque FJ (2009) Novel donepezil-based inhibitors of acetyl- and butyrylcholinesterase and acetylcholinesterase-induced β -amyloid aggregation. *J Med Chem* 51:3588–3598
- Candeias E, Duarte AI, Carvalho C, Correia SC, Cardoso S, Santos RX, Plácido AI, Perry G, Moreira PI (2012) The impairment of insulin signaling in Alzheimer's disease. *IUBMB Life* 64(12):951–957
- Catto M, Berezin AA, Lo Re D, Loizou G, Demetriades M, De Stradis A, Campagna F, Koutentis PA, Carotti A (2012) Design, synthesis and biological evaluation of benzo[e][1,2,4]triazin-7(1*H*)-one and [1,2,4]-triazino[5,6,1-*jk*]carbazol-6-one derivatives as dual inhibitors of beta-amyloid aggregation and acetyl/butyryl cholinesterase. *Eur J Med Chem* 58:84–97
- Chen Y, Su J, Fang L, Liu M, Peng s, Liao H, Lehmann J, Zhang Y (2012) Tacrineferulic acid-nitric oxide (NO) donor trihybrids as potent, multifunctional acetyl and butyrylcholinesterase inhibitors. *J Med Chem* 55:4309–4321
- Cheung J, Rudolph MJ, Burshteyn F, Cassidy MS, Gary EN, Love J, Franklin MC, Height JJ (2012) Structures of human acetylcholinesterase in complex with pharmacologically important ligands. *J Med Chem* 55:10282–10286
- Chiou SY, Huang CF, Hwang MT, Lin G (2009) Comparison of active sites of butyrylcholinesterase and acetylcholinesterase based on inhibition by geometric isomers of benzene-di-*N*-substituted carbamates. *Mol Toxicol* 23:303–308
- Costanzo P, Cariati L, Desiderio D, Sgammato R, Lamberti A, Arcone R, Salerno R, Nardi M, Masullo M, Oliverio M (2016) Design, synthesis, and evaluation of donepezil-like compounds as AChE and BACE-1 inhibitors. *ACS Med Chem Lett* 7:470–475
- Cummings JL, Morstorf T, Zhong K (2007) Alzheimer's disease drug-development pipeline: few candidates, frequent failures. *Alzheimers Res Ther* 6:1–7
- Delogu GL, Matos MJ, Fanti M, Era B, Medda R, Pieroni E, Fai A, Kumar A, Pintus F (2016) 2-Phenylbenzofuran derivatives as butyrylcholinesterase inhibitors: Synthesis, biological activity and molecular modeling. *Bioorg Med Chem Lett* 26:2308–2313
- Dvir H, Silman I, Harel M, Rosenberry TL, Sussmana JL (2010) Acetylcholinesterase: from 3D structure to function. *Chem Biol Interact* 187:10–22
- Ellman GL, Courtney KD, Andres V, Featherstone RM (1961) A new and rapid colorimetric determination of acetylcholinesterase activity. *Biochem Pharm* 7:88–95
- Friesner RA, Banks JL, Murphy RB, Halgren TA, Klicic JJ, Mainz DT, Repasky MP, Knoll EH, Shelley M, Perry JK (2004) Glide: a new approach for rapid, accurate docking and scoring. 1. Method and assessment of docking accuracy. *J Med Chem* 47:1739–1749
- Friesner RA, Murphy RB, Repasky MP, Frye LL, Greenwood JR, Halgren TA, Sanschagrin PC, Mainz DT (2006) Extra precision glide: docking and scoring incorporating a model of hydrophobic enclosure for protein-ligand complexes. *J Med Chem* 49:6177–6196
- Gilhus NE, Skeie GO, Romi F, Lazaridis K, Zisimopoulou P, Tzartos S (2016) Myasthenia gravis - autoantibody characteristics and their implications for therapy. *Nat Rev Neurol* 12(5):259–268
- Groner E, Ashani Y, Schorer-Apelbaum D, Sterling J, Herzig Y, Weinstock M (2007) The kinetics of inhibition of human acetylcholinesterase and butyrylcholinesterase by two series of novel carbamates. *Mol Pharmacol* 71(6):1610–1617
- Halgren TA, Murphy RB, Friesner RA, Beard HS, Frye LL, Pollard WT, Banks JL (2004) Glide: a new approach for rapid, accurate docking and scoring. 2. Enrichment factors in database screening. *J Med Chem* 47:1750–1759
- Huang L, Su T, Shan W, Luo Z, Sun Y, He F, Li X (2012) Inhibition of cholinesterase activity and amyloid aggregation by berberine-phenyl-benzoheterocyclic and tacrine-phenyl-benzoheterocyclic hybrids. *Bioorg Med Chem* 20:3038–3048
- Jiang H, Wang X, Huang L, Luo Z, Su T, Ding K, Lia X (2011) Benzenediol-berberine hybrids: Multifunctional agents for Alzheimer's disease. *Bioorg Med Chem* 19:7228–7235
- Kneza D, Brusa B, Coquelles N, Sosića I, Šinka R, Brazzolotto X, Mravljaka J, Colletierb JP, Gobeca S (2015) Structure-based development of nitroxoline derivatives as potential multifunctional anti-Alzheimer agents. *Bioorg Med Chem* 23:4442–4452
- Leon J, Marco-Contelles J (2011) A step further towards multitarget drugs for Alzheimer and neuronal vascular diseases: targeting the cholinergic system, amyloid- β aggregation and Ca^{2+} dyshomeostatis. *J Curr Med Chem* 18:552
- Li B, Duysen EG, Carlson M, Lockridge O (2008) The butyrylcholinesterase knockout mouse as a model for human

- butyrylcholinesterase deficiency. *J Pharmacol Exp Ther* 324:1146–1154
- Mehta M, Adem A, Sabbagh M (2012) New acetylcholinesterase inhibitors for Alzheimer's disease. *Int J Alzheimers Dis*. doi:10.1155/2012/728983
- Mesulam MM, Guillozet A, Shaw P, Levey A, Duysen E, Lockridge O (2002) Acetylcholinesterase knockouts establish central cholinergic pathways and can use butyrylcholinesterase to hydrolyze acetylcholine. *Neuroscience* 110:627–639
- Nachon F, Carletti E, Ronco C, Trovaslet M, Nicolet Y, Jean L, Renard PY (2013) Crystal structures of human cholinesterases in complex with huprine W and tacrine: elements of specificity for anti-Alzheimer's drugs targeting acetyl- and butyrylcholinesterase. *Biochem J* 453:393–399
- Nagle P, Pawar Y, Sonawane A, Bhosale S, More D (2014) Docking simulation, synthesis and biological evaluation of novel pyridazinone containing thymol as potential antimicrobial agents. *Med Chem Res* 23:918–926
- Nepovimova E, Uliassi E, Korabecny J, Peña-Altamira LE, Samez S, Pesaresi A, Garcia GE, Bartolini M, Andrisano V, Bergamini C, Fato R, Lamba D, Roberti M, Kuca K, Monti B, Bolognesi ML (2014) Multitarget drug design strategy: quinone–tacrine hybrids designed To block Amyloid- β aggregation and to exert anticholinesterase and antioxidant effects. *J Med Chem* 57(20):8576–8589
- Nicolet Y, Lockridge O, Masson P, Fontecilla-Camps JC, Nachon F (2003) Crystal structure of human butyrylcholinesterase and of its complexes with substrate and products. *J Biol Chem* 278:41141–41147
- Orhan I, Aslan S, Kartal M, Şener B, Başer KHC (2008) Inhibitory effect of Turkish *Rosmarinus officinalis* L. on acetylcholinesterase and butyrylcholinesterase enzymes. *Food Chem* 108:663–668
- Otto R, Penzis R, Gaube F, Winckler T, Appenroth D, Fleck C, Treankle C, Lehmann J, Enzensperger C (2014) Enzensperger, Beta and gamma carboline derivatives as potential anti-Alzheimer agents: a comparison. *Eur J Med Chem* 87:63–70
- Önkol T, Gökçe M, Orhan İ, Kaynak F (2013) Design, synthesis and evaluation of some novel 3(2H)-pyridazinone-2-yl acetohydrazides as acetylcholinesterase and butyrylcholinesterase inhibitors. *Org Commun* 6:55–67
- Özçelik AB, Gökçe M, Orhan İ, Kaynak F, Şahin MF (2010) Synthesis and antimicrobial, acetylcholinesterase and butyrylcholinesterase inhibitory activities of novel ester and hydrazide derivatives of 3(2H)-pyridazinone. *Arzneim Forsch* 60(7):452–458
- Rathish IG, Javed K, Ahmad S, Bano S, Alam MS, Akhter M, Pillai KK, Ovais S, Samim M (2012) Synthesis and evaluation of anticancer activity of some novel 6-aryl-2-(p-sulfamylphenyl)-pyridazin-3(2H)-ones. *Eur J Med Chem* 49:304–309
- Romero A, Cabelos R, Oset-Gasque MJ, Samadi A, Marco-Contelles J (2013) Novel tacrine-related drugs as potential candidates for the treatment of Alzheimer's disease. *Bioorg Med Chem Lett* 23(7):1916–1922
- Saeed A, Mahesara PA, Zaib S, Khanb MS, Matinc A, Shahidd M, Iqbal J (2014) Synthesis, cytotoxicity and molecular modelling studies of new phenylcinnamide derivatives as potent inhibitors of cholinesterases. *Eur J Med Chem* 78:43–53
- Saeed A, Zaib S, Ashraf S, Iftikhar J, Muddassar M, Zhang KYJ, Iqbal J (2015) Synthesis, cholinesterase inhibition and molecular modelling studies of coumarin linked thiourea derivatives. *Bioorg Chem* 63:58–63
- Samadi A, De los Ríos C, Bolea I, Chioua M, Iriepa I, Moraleda I, Bartolini M, Andrisano V, Galvez E, Valderas C, Unzeta M, Marco-Contelles J (2012) Multipotent MAO and cholinesterase inhibitors for the treatment of Alzheimer's disease: synthesis, pharmacological analysis and molecular modeling of heterocyclic substituted alkyl and cycloalkyl propargyl amine. *Eur J Med Chem* 52:251–262
- Shah MS, Khan SU, Ejaz SA, Afridi S, Rizvi SUF, Najam-ul-Haq M, Iqbal J (2016) Cholinesterases inhibition and molecular modeling studies of piperidyl-thienyl and 2-pyrazoline derivatives of chalcones. *Biochem Biophys Res Commun* xxx:1–10
- Siddiqui AA, Mishra R, Shaharyar M (2010) Synthesis, characterization and antihypertensive activity of pyridazinone derivatives. *Eur J Med Chem* 45:2283–2290
- Siddiqui AA, Mishra R, Shaharyar M, Husain A, Rashid M, Pal P (2011) Triazole incorporated pyridazinones as a new class of antihypertensive agents: Design, synthesis and in vivo screening. *Bioorg Med Chem Lett* 21:1023–1026
- Simoni E, Daniele S, Bottegani G, Pizzirani D, Trincavelli ML, Goldoni L, Tarozzo G, Reggiani A, Martini C, Piomelli D, Melchiorre C, Rosini M, Cavalli A (2012) Combining Galantamine and Memantine in Multitargeted, New Chemical Entities Potentially Useful in Alzheimer's Disease. *J Med Chem* 55(22):9708–9721
- Strelnik AD, Petukhov AS, Zueva AV, Zobov VV, Petrov KA, Nikolsky EE, Balakin KV, Bachurin SO, Shtyrin YG (2016) Novel potent pyridoxine-based inhibitors of AChE and BChE, structural analogs of pyridostigmine, with improved in vivo safety profile. *Bioorg Med Chem Lett* 26:4092–4094
- Şahin MF, Badıçoğlu B, Gökçe M, Küpeli E, Yeşilada E (2004) Synthesis and analgesic and antiinflammatory activity of methyl [6-substitue-3(2H)-pyridazinone-2-yl]acetate derivatives. *Arch Pharm Pharm Med* 33:445–452
- Tampi RR, Tampi DJ, Ghori AK (2016) Acetylcholinesterase inhibitors for delirium in older adults. *Am J Alzheimer Dis* 31(4):305–310
- Tougu V (2001) Acetylcholinesterase: mechanism of catalysis and inhibition. *Curr Med Chem Cent Nerv Syst Agents* 1:155–170
- Utku S, Gökçe M, Aslan G, Bayram G, Ülger M, Emekdaş G, Şahin MF (2011a) Synthesis and in vitro antimycobacterial activities of novel 6-substituted-3(2H)-pyridazinone-2-acetyl-2-(substituted/nonsubstituted acetophenone)hydrazones. *Turk J Chem* 35:331–339
- Utku S, Gökçe M, Orhan İ, Şahin MF (2011b) Synthesis of novel 6-substituted-3(2H)-pyridazinone-2-acetyl-2-(substituted/non-substituted benzal)hydrazones derivatives and acetylcholinesterase and butyrylcholinesterase inhibitory activities in vitro. *Arzneim Forsch* 61:1–7
- Williams P, Sorribas A, Howes M-JR (2011) Natural products as a source of Alzheimer's drug leads. *Nat Prod Rep* 28:48–77
- Xing W, Fu Y, Shi Z, Lu D, Zhang H, Hu Y (2013) Discovery of novel 2,6-disubstituted pyridazinone derivatives as acetylcholinesterase inhibitors. *Eur J Med Chem* 63:95–103
- Yamali C, Ozan GH, Kahya B, Çobanoğlu S, Şüküroğlu MK, Doğruer DS (2015) Synthesis of some 3(2H)-pyridazinone and 1(2H)-phthalazinone derivatives incorporating aminothiazole moiety and investigation of their antioxidant, acetylcholinesterase, and butyrylcholinesterase inhibitory activities. *Med Chem Res* 24:1210–1217
- Zha X, Lamba D, Zhang L, Lou Y, Xu C, Kang D, Chen L, Xu Y, Zhang L, De Simone A, Samez S, Pesaresi A, Stojan J, Lopez MG, Egea J, Andrisano V, Bartolini M (2016) Novel tacrine-benzofuran hybrids as potent multitarget-directed ligands for the treatment of Alzheimer's disease: design, synthesis, biological evaluation and X-ray crystallography. *J Med Chem* 59:114–131
- Zhou Y, Wang S, Zhang Y (2010) Catalytic reaction mechanism of acetylcholinesterase determined by born-oppenheimer AB initio QM/MM molecular dynamics simulations. *J Phys Chem B* 114:8817–8825